Connectomics and Cognition Define a Treatment-Resistant Form of Post-Traumatic Stress Disorder

Amit Etkin [1, 2, 3, 4, 20, §], Adi Maron-Katz[1, 2, 3, 4, 20], Wei Wu [1, 2, 3, 4, 5, 20], Gregory A. Fonzo[1, 2, 3, 4, 20], Julia Huemer[1, 2, 3, 20], Petra E. Vértes[7, 20], Brian Patenaude[1, 2, 3, 4], Jonas Richiardi[10,11], Madeleine S. Goodkind[12,13], Corey J. Keller[1, 2, 3, 4], Jaime Ramos-Cejudo[4, 6], Yevgeniya V. Zaiko[1, 2, 3], Kathy K. Peng [1,3], Emmanuel Shpigel[1,2,3,4], Parker Longwell[1,2,3,4], Russ T. Toll [1, 2, 3, 4], Allison Thompson[1], Sanno Zack[1], Bryan Gonzalez[4, 6], Raleigh Edelstein[1,2,3,4], Jingyun Chen[4, 6], Irene Akingbade[1,3,4], Elizabeth Weiss[1,3], Roland Hart[4, 6], Silas Mann[4, 6], Kathleen Durkin[4, 6], Steven Baete[4, 12, 13], Fernando Boada[4, 14, 15], Afia Genfi[4, 6], Jillian Autea [1,2,3,4], Jennifer Newman[4, 6] Desmond J. Oathes[16], Steven E. Lindley[1,3], Duna Abu-Amara[4, 6], Bruce A. Arnow[1], Nicolas Crossley[17, 18], Joachim Hallmayer[1, 2, 3], Silvia Fossati[4, 6], Barbara O. Rothbaum[19], Charles R. Marmar[4, 6], Edward T. Bullmore[7, 8, 9], Ruth O'Hara,[1, 3]

[1]Department of Psychiatry and Behavioral Sciences
[2]Stanford Neurosciences Institute
Stanford University, Stanford, CA, 94304, USA
[3]Veterans Affairs Palo Alto Healthcare System, and the Sierra Pacific Mental Illness, Research, Education, and Clinical Center (MIRECC), Palo Alto, CA, 94394, USA
[4]Steven and Alexandra Cohen Veterans Center for Post-traumatic Stress and Traumatic Brain Injury, New York University Langone School of Medicine, New York, NY 10016, USA
[5]School of Automation Science and Engineering, South China University of Technology, Guangzhou, Guangdong 510640, China
[6]Department of Psychiatry, New York University Langone School of Medicine, New York, NY 10016, USA
[7]University of Cambridge, Behavioral & Clinical Neuroscience Institute, Department of Psychiatry, Cambridge CB2 0SZ, UK
[8]Cambridgeshire and Peterborough NHS Foundation Trust, Cambridge CB21 5EF, UK
[9]GlaxoSmithKline, ImmunoPsychiatry, Alternative Discovery and Development, Stevenage SG1 2NY, UK
[10]Department of Medical Radiology, Lausanne University Hospital, Lausanne, Switzerland
[11]Advanced Clinical Imaging Technology, Siemens Healthcare AG, Lausanne, Switzerland
[12]New Mexico Veterans Affairs Healthcare System, Albuquerque, NM, 87108, USA

[13]Department of Psychiatry and Behavioral Sciences, University of New Mexico, Albuquerque, NM, 87131, USA
[14] Center for Advanced Imaging Innovation and Research (CAI2R), NYU School of Medicine, New York, NY, USA
[15] Center for Biomedical Imaging, Dept of Radiology, NYU School of Medicine, New York, NY, USA
[16]Center for Neuromodulation in Depression and Stress, Department of Psychiatry, University of Pennsylvania Perelman School of Medicine, Philadelphia, Pennsylvania 19104, USA
[17] Department of Psychiatry, School of Medicine, Pontificia Universidad Católica de Chile, 6513677 Santiago, Chile
[18]Department of Psychosis Studies, Institute of Psychiatry, Psychology and Neuroscience, King's College London, London SE5 8AF, UK
[19]Trauma and Anxiety Recovery Program, Department of Psychiatry, Emory University School of Medicine, Atlanta, GA, USA

[20] Equal contributions

§ Corresponding author:
Amit Etkin,
Department of Psychiatry and Behavioral Sciences
Stanford University
401 Quarry Road, MC: 5797
Stanford, CA 94305-5797
Email: amitetkin@stanford.edu
Phone: +1 650-725-5736

One sentence summary
This study identifies a reproducible, objective, biobehavioral phenotype within the broader clinical syndrome of PTSD, which characterizes a patient subgroup that fails to respond to the best-supported treatment, and is associated with specific impairments in neurostimulation-evoked neural signal flow.

Abstract

A mechanistic understanding of psychopathology has been hampered by extensive heterogeneity of biology, symptoms, and behavior within subjectively-defined diagnostic categories. We investigated whether leveraging individual differences in core information processing impairments associated with post-traumatic stress disorder (PTSD) patients could reveal biophenotypes within the disorder that are clinically- and mechanistically-relevant. We found that a subgroup of PTSD patients from two independent cohorts displayed both aberrant functional connectivity within the ventral attention network (VAN) and impaired verbal memory – despite the substantial clinical/demographic differences between the cohorts. This combined phenotype was not associated with differences in current symptoms or comorbidities, but nonetheless predicted resistance to psychotherapy, the best-validated treatment for PTSD. Using concurrent focal non-invasive transcranial magnetic stimulation (TMS) and electroencephalography we then identified alterations in neural signal flow in the VAN evoked by direct stimulation of that network that were associated with these individual differences in within-VAN functional connectivity. Our findings thus leverage objective neurobiological mechanisms to define an otherwise clinically-latent but prognostically-relevant phenotype within the broader clinical syndrome of PTSD. This approach promotes a transition from a purely descriptive characterization of psychopathology to one with enhanced inferential power by virtue of direct perturbation of circuit dynamics, which directly inform targets for remediation through plasticity-inducing brain stimulation treatments.

Introduction

Extreme stress can exert long-lasting detrimental effects and is a precipitant of numerous manifestations of psychopathology in humans. The most severe of these is post-traumatic stress disorder (PTSD), a common, chronic and disabling mental illness whose pathophysiology is both complex and poorly understood. PTSD, like all psychiatric disorders, is currently diagnosed based on different combinations of clinical symptoms (*1, 2*). As a consequence of this symptom-based diagnostic framework, the syndrome of PTSD contains extensive clinical heterogeneity, covering hundreds of thousands of different symptom combinations (*3-5*). Moreover, despite many years of pioneering work characterizing the brains, behavior and physiology of individuals with PTSD, we still lack biological metrics for consistently partitioning clinical variation within the broad clinical syndrome of PTSD in a way that has both mechanistic implications for understanding disorder expression as well as demonstrable clinical relevance for the practitioner. Establishment of such metrics could provide a basis for targeted treatment selection and development of novel therapeutics, much as has been achieved in other areas of biology and medicine (*6*).

Our approach draws on the premise that disruption in basic brain information-processing functions underlying cognition form the foundation upon which various aspects of PTSD are built. For example, impaired declarative memory in PTSD, most evident for verbal learning and memory (*7*), may contribute to development of perturbed emotional memories acquired as a result of PTSD-producing traumas (*8, 9*), and is relevant for treatment outcome (*7, 9-12*). Memory intrusions are a classic PTSD symptom and memory is a primary target for evidence-based treatments utilizing therapeutic exposure. Similarly, impairments in attention and higher-level executive functions may result in difficulty disengaging from trauma-relevant stimuli and engaging with the task at hand (*13*). Moreover, we expect that since only some PTSD patients display impaired cognition when compared with healthy individuals, the associated neural abnormalities will likewise be evident in only a portion of patients. As such, cognitive deficits may allow us to understand clinically-meaningful heterogeneity in PTSD by providing an opportunity to link dysfunction(s) in core brain processes to the neurobiology of information-processing systems (*10*), and from there to account for heterogeneity in symptoms or treatment outcome.

At the neural level, widespread interactions within and across distributed brain networks are well-documented to underlie cognitive processes (*14-19*). Individual differences in cognitive capacities have in turn been related to individual differences in connectivity of the fronto-parietal, default-mode, dorsal attention and ventral attention (i.e. “salience”) networks using functional magnetic resonance imaging (fMRI), even under task-free resting-state conditions in healthy individuals (*20, 21*). Neuroimaging studies in PTSD have also identified resting-state fMRI connectivity abnormalities in these large-scale neural networks in individuals with PTSD (*22-24*). As a clinical biomarker tool, resting-state connectivity carries additional advantages, such as its ease of semi-standardized acquisition and independence of performance requirements. Thus, examining deficits in cognition and related resting-state network interactions may help objectively define clinically-relevant phenotypes within the larger clinical syndrome of PTSD. This would further ground aspects of clinical heterogeneity in biological

mechanisms. Additionally, use of resting-state connectivity facilitates generalization of our findings given that collection of these data is now commonplace in semi-standardized ways across human imaging studies.

Resting-state connectivity has been a major area of biomarker-related research because it has been presumed that abnormalities in resting-state fMRI connectivity reflect alterations in the interaction between different brain regions (i.e. in direct information flow)(*25*). However, due to the limitations of conventional neuroimaging with respect to causal inference, the relationship between identified abnormalities in network interactions in patients (e.g. using resting-state fMRI) and affected components of neural signal flow mechanisms has remained largely unknown. Not only is this knowledge important for understanding the meaning of resting-state fMRI connectivity, but also for driving a transition from a descriptive approach to mental illness to a circuit-based mechanistic one that could also be used to directly guide much-needed novel interventions (*26*). One way to address this challenge is to directly and non-invasively stimulate cortical regions using single pulses of transcranial magnetic stimulation (spTMS) while recording consequent brain activity with electroencephalography (EEG), thereby allowing interrogation of stimulation-evoked neural signal flow at a neural temporal scale (*27-31*). Each TMS pulse produces a series of EEG responses. Early phase-locked potentials (e.g. at 30ms) likely reflect evoked excitatory activity, while later potentials (~50-400ms) likely reflect a slow inhibitory rebound to stimulation unfolding over several hundred milliseconds (*30, 32-35*). Changes in oscillatory power can outlast the phase-locked potentials, for which inhibitory processes have also been implicated (*36*). By stimulating various cortical regions with concurrent spTMS/EEG one can therefore relate stimulation-driven effects on signal flow to differences in fMRI connectivity, thus grounding our understanding of fMRI connectivity in more specific neurophysiological mechanisms using non-invasive neurostimulation. As such, not only does concurrent spTMS/EEG offer an opportunity to understand how direct stimulation-evoked neural signal flow is associated with fMRI connectivity, but it also establishes brain loci and neurophysiological signals that may in turn become targets for remediation through plasticity-inducing repetitive TMS-based treatment.

In the current study we therefore investigated the biology underlying heterogeneity within the broader PTSD clinical syndrome by: 1) identifying how deficits in basic cognitive functioning relate to abnormalities in resting-state fMRI connectivity in cognitive networks, thereby facilitating broad and maximally-generalizable inference regarding aspects of network function underlying information-processing dysfunction; 2) testing whether phenotypes defined through cognition and network connectivity generalize across demographically and clinically-distinct PTSD populations, 3) delineating the clinical relevance of these phenotypes by examining their relationship to both individual differences in symptom expression as well as individual differences in capacity to benefit from evidence-based treatment, and 4) interrogating alterations in neurostimulation-evoked neural signal flow using concurrent spTMS/EEG, which may underlie and help explain individual differences in network biophenotypes. Figure 1 shows an overview of the experimental design.

Results

Mapping brain to behavioral deficits in PTSD

The core hypothesis driving our analytic approach is that clinically-meaningful biological heterogeneity within the broader clinical syndrome of PTSD can be understood by contrasting brain functional data (here with resting-state fMRI; Figure 2a) from patients with demonstrable information-processing i.e. cognitive impairments against functional data from healthy individuals and cognitively-intact patients with PTSD. We began by comparing performance on a battery of computerized neurocognitive tasks in healthy individuals and PTSD patients from Study 1 (see sample characteristics in tables S1 and S2). Given prior meta-analytic investigations of neurocognitive functioning in PTSD, we expected patients to show deficits in verbal learning and memory, attention, working memory, information processing speed and various executive functions (e.g. inhibition and flexibility)(*7*). To maximize the interpretability of our findings, we furthermore selected only unmedicated PTSD patients (N=36 healthy controls; N=56 patients). Looking at deficits in patients with respect to healthy individuals, only verbal memory delayed recall demonstrated a significant difference after controlling for a false discovery rate (FDR) of 0.05 (Wald χ^2=6.0, p=0.014, pFDR=0.0431; Figures 2b and S1). This small to medium effect size (Cliff's delta=0.23) is consistent with that reported in a meta-analyses of neurocognition in PTSD(*7*). Since our goal was to identify a candidate cognitive phenotype for dissecting heterogeneity within PTSD, we created a cutoff in delayed recall scores using a discriminant function that determined the optimal value for differentiating patients from healthy individuals. Patients with delayed recall scores below this cutoff (90% accuracy or lower; 26% of PTSD cases, see supplemental results) were considered to be impaired relative to healthy individuals, while patients performing above this cutoff were considered to be cognitively intact. These groupings were then used for analysis of the neuroimaging data in both Study 1 and Study 2.

We next examined whether functional connectivity abnormalities were observed selectively for the memory-impaired PTSD subgroup in resting-state fMRI analyses. Functional connectivity was calculated for each pair of cortical regions in a previously-identified set of seven canonical cortical connectivity networks (*37, 38*)(Figure 2a). Pairwise connectivity values were then averaged based on region-network assignments to obtain one within-network connectivity value for each network and one between-networks connectivity value for each pair of networks. These measures were then entered into a 3-level group factor generalized linear model (i.e. verbal memory impaired PTSD (N=12), verbal memory intact PTSD (N=39), healthy (N=36)), while controlling for age, gender, education and head motion. After FDR correction for all pairwise network-level connections, only connectivity within the ventral attention network (VAN) was found to differ among the three groups (Figure 2c; Wald χ^2=14.8, p=0.0006, p_{FDR}=0.015). This network consists of parcels located in the insula, dorsal anterior cingulate, anterior middle frontal gyrus and supramarginal gyrus. A subsequent post-hoc pairwise contrast between the groups (using a Sidak correction for multiple comparisons) revealed that the impaired PTSD group had lower within-VAN connectivity relative to both healthy individuals (p=0.0001) and the intact PTSD group (p=0.03), while cognitive-intact patients with PTSD and healthy individuals did not differ. These

findings were not confounded by age, intelligence or performance on other cognitive tests (see supplemental results).

We next tested whether the brain-behavior findings in PTSD patients found in Study 1 could generalize to a new cohort of patients and healthy controls. Study 1 used DSM-IV for diagnosis of PTSD and was composed primarily of civilians, was largely female, was all right-handed, featured patients who developed PTSD most commonly after physical or sexual assault, and used spiral in-out imaging. Moreover, only unmedicated patients were used in our primary analyses in Study 1. By contrast, Study 2 used DSM-5 for diagnosis of PTSD and was composed entirely of Iraq/Afghanistan era military combat-exposed Veterans, was overwhelmingly male, included left-handed individuals, featured patients who developed PTSD almost exclusively after combat-related events (N=117 healthy controls; N=128 PTSD participants), and used echoplanar imaging. Study 2 patients were also more frequently medicated (representing a broader variety of medications as well; see Tables S1 and S2). Thus, given predominant demographic differences, but similar neurocognitive and neuroimaging methodological approaches, the Study 2 sample represents a prime opportunity for testing the generalization of our brain-behavior findings from Study 1. The verbal memory impairment was also significantly more frequent amongst the PTSD group than healthy controls in Study 2 (33% of cases; Fisher's exact test p=0.018; N=117 healthy controls; N=40 memory-impaired PTSD; N=83 memory-intact PTSD).

We next examined the relationship of these a priori-derived verbal memory-based groupings on within-VAN fMRI connectivity in Study 2. Using the generalized linear models and covariates defined in Study 1, while additionally controlling for acquisition site, the different medication classes represented in our population and handedness, we found a significant effect of verbal memory-based grouping on within-VAN connectivity (Figure 3a; Wald χ^2=11.4, p=0.003). Specifically, within-VAN connectivity was significantly lower in verbal memory-impaired PTSD cases, relative to healthy individuals (p=0.042) and verbal memory-intact PTSD cases (p=0.002), after Sidak correction for multiple comparisons. Similarly, when considering all within- and between-network connections, the within-VAN connectivity effect also passed the FDR significance threshold (Figure 3b; p_{FDR}=0.009). These results were likewise not confounded by age, intelligence or performance on other cognitive tasks (see supplemental results).

In summary, we found that a biobehavioral phenotype consisting of impaired delayed recall of verbal memory and blunted within-VAN resting state fMRI connectivity exists within the larger clinical syndrome of PTSD. This finding was observed in two independent cohorts, and was not related to potential confounding variables.

Determining the clinical significance of impaired verbal memory and poor within-VAN connectivity: current symptoms and comorbidities

We next asked whether clinical aspects of PTSD, or its common comorbidities, differed in patients as a function of verbal memory delayed recall, within-VAN connectivity or their interaction. As detailed in supplemental results and Figure S2, we found no relationships of any of these variables, across either Study 1 or 2, to PTSD or depression severity (including PTSD symptom clusters and dissociative symptoms),

comorbid diagnoses, alcohol use, traumatic brain injury or quality of life. As such, it appears that, from a cross-sectional clinical perspective, the cognitive biobehavioral phenotype we have identified within the clinical syndrome of PTSD cannot be distinguished by current symptoms or comorbidities (i.e. clinically "latent"). We therefore next asked whether this phenotype was predictive of clinical outcome when PTSD patients are treated with the best-supported intervention for the disorder – exposure-based psychotherapy.

Determining the clinical significance of impaired verbal memory and poor within-VAN connectivity: treatment outcome prediction

Trauma-focused psychotherapy, such as prolonged exposure, is considered the gold-standard treatment for PTSD (superior to medications) and centrally involves therapeutic techniques that tap learning and memory (*12, 39*). Within Study 1, 66 patients entered a randomized clinical trial contrasting prolonged exposure (PE; N=36) psychotherapy to a wait-list (WL; N=30) control arm, in order to understand the brain mechanisms underlying PE (Figure S3)(*40, 41*). As expected (*39*), PE resulted in a much greater reduction in PTSD symptoms, as assessed by the DSM-IV CAPS, than WL ($F(2,113)=20.0$, $p= 4x10^{-8}$; Table S4), with no difference in dropout rates (Fisher's exact test p=0.14).

Using generalized linear mixed models in an intent-to-treat analysis, we next examined the potential moderating effects of verbal memory delayed recall and within-VAN functional connectivity (i.e. whether these factors differentially predicted outcome with PE versus WL, as tested by a moderator by group by time interaction). When examined alone, neither verbal memory delayed recall impairment nor within-VAN functional connectivity significantly moderated treatment outcome (memory: $F(2,90)=2.0$, p=0.13; connectivity: $F(2,108)=0.2$, p=0.84). By contrast, when examined in interaction, there was a strongly significant moderation effect on treatment outcome as a function of both verbal memory impairment and within-VAN connectivity ($F(2,82)=27.4$, $p<10^{-8}$; Figure 4a shows a median split on connectivity scores to illustrate the mixed model result). This model explained more treatment outcome variance than either single variable model alone (likelihood ratio test: $\Delta G^2=102.8$, df=6, p<0.001). Moreover, when considering all within- and between-network connections, the moderation effect for within-VAN connectivity is also significant after FDR correction for multiple comparisons (Figure 4b; $p_{FDR}=10^{-7}$). When testing each arm alone, we found that significant outcome prediction as a function of both memory and connectivity was found only in the PE arm (PE: $F(1,41)=187.8$, $p<10^{-8}$; WL: $F(1,41)=1.0$, p=0.31). These effects were unrelated to any demographic variables, medication use or baseline PTSD severity, and had individual-level predictive value (see supplemental results).

As seen in Figure 4a, the significant interaction in the PE arm arose from the poor treatment response of individuals with both impaired verbal memory and lower levels of within-VAN connectivity. Having either intact verbal memory or normal levels of within-VAN connectivity resulted in a robust treatment response. For context, a CAPS-IV cutoff of 20 is considered symptom remission (*42*), which many of the individuals without both the memory and connectivity impairments were able to achieve. Thus, the

biological stratification within the broader PTSD clinical syndrome discovered here is of clinical significance.

Identifying the relationship of within-VAN fMRI connectivity to mechanisms of direct neurostimulation-evoked neural influence using spTMS/EEG

Though resting-state fMRI connectivity is a broadly-used measure in both basic and clinical human neuroscience, which helped motivate our examination of this metric in this study, its physiological meaning remains unclear. That is, it is largely unknown how aspects of neurophysiology and directed information flow (as revealed by neurostimulation-evoked circuit perturbations) are reflected in individual differences in fMRI connectivity. By stimulating various cortical regions with concurrent spTMS/EEG one can discover the directional influence of the stimulated region on downstream regions (as contrasted with solely correlation-based connectomic mapping). We therefore next sought to understand neurophysiological mechanisms that may account for variations in within-VAN connectivity. For this goal, we conducted concurrent spTMS/EEG circuit interrogation by stimulating a TMS-accessible region of the VAN, located in the anterior middle frontal gyrus (aMFG(VAN); Figure 5a). We contrasted results of VAN spTMS with stimulation of a nearby region in the posterior middle frontal gyrus located within the fronto-parietal control network (pMFG(FPCN); Figure 5a), also termed the executive control network. Importantly, in prior work using concurrent spTMS/fMRI, we found that spTMS to the right aMFG(VAN) node resulted in increased within-VAN fMRI connectivity relative to spTMS to the right pMFG(FPCN) node (*43*). Here we localized the VAN and FPCN nodes for neuronavigation in the same manner as our prior work, though now both left-sided and right-sided spTMS sites were included. These experiments were added to Study 2 after acquisition of fMRI and behavioral data had begun, thus a majority but not all participants underwent both fMRI and spTMS/EEG.

As discussed in the introduction, EEG quantification of directed neural influence includes both phase-locked amplitude changes (TMS-evoked responses (TERs)) as well as changes in power of different frequency bands (event-related spectral perturbation (ERSP) changes). In order to cast a broad net across spTMS/EEG-revealed neurophysiological mechanisms, we examined a broad range of TER measures (potentials at 30, 60, 100, and 200ms after the TMS pulse) and ERSP measures (across theta, alpha, beta and low gamma frequency ranges and in time bins extending up to 800ms after the TMS pulse; Figure 5b). These were extracted from a spatial mask covering VAN regions using an EEG source localization algorithm (*44*). We then correlated each individual's within-VAN resting-state fMRI connectivity against each of the VAN-extracted TER and ERSP measures, correcting for multiple comparisons with FDR across the full set of correlations (i.e. each of four stimulation sites and all EEG measures). These analyses were done on participants in Study 2, a portion of whom additionally underwent spTMS/EEG (which was added after study recruitment had begun). As shown in Table S5, there were no demographic differences between those Study 2 patients who did and did not have spTMS/EEG data.

Furthermore, spTMS/EEG data were processed by an automated artifact rejection algorithm we recently developed (*31*), thereby minimizing the biases in preprocessing possible with manual rejection of artifacts, as is typically done in prior spTMS/EEG research.

After quality control of processed spTMS/EEG data (see methods) we had ~110 participants with both spTMS/EEG and resting-state fMRI data across both healthy and PTSD groups (right aMFG(VAN) N=52 healthy/58 PTSD, left aMFG(VAN) N=50/63, right pMFG(FPCN) N=56/64, left pMFG(FPCN) N=50/48). Correlation analyses between fMRI connectivity and spTMS/EEG response were done across both healthy individuals and patients in order to identify generalizable neurostimulation-evoked neural influence signals in the spTMS/EEG data that may account for within-VAN fMRI connectivity, under the assumption that such a relationship is not specific to a distinct clinical diagnosis. We subsequently tested whether clinical group moderated these findings.

As seen in Figure 5c, multiple relationships between within-VAN fMRI connectivity and spTMS/EEG measures survived FDR correction, all of which were in response to stimulation of the right aMFG(VAN) node. All of these relationships were positive correlations and related to ERSP measures occurring largely after the phase-locked TER ended. For example, as illustrated in Figure 5d, those individuals with lower within-VAN fMRI connectivity displayed profound VAN-localized alpha desynchronization (i.e. reduction in alpha power below baseline (defined as -300 to -100ms)) in the 400-600ms post-spTMS pulse period, while those with higher fMRI connectivity showed either more modest or no desynchronization. To visualize these multiple fMRI-spTMS/EEG relationships, we show in Figure 5e ERSP plots for the individuals in the top third of the within-VAN fMRI connectivity distribution and those within the bottom third. As can be seen, there is profound and prolonged desynchronization in individuals with lower levels of within-VAN fMRI connectivity extending until the end of the 800ms time period across which we quantified ERSP measures. Put differently, while a neurophysiological response to a spTMS pulse ended by ~400ms for individuals with higher within-VAN connectivity, it persisted for at least 800ms in those with lower within-VAN connectivity.

These fMRI connectivity-spTMS/EEG relationships were unchanged if we accounted for diagnostic group (healthy versus PTSD; Wald χ^2's>8.4, p's<0.004). Moreover, these findings were specific for the right aMFG(VAN) stimulation site. Covarying for the equivalent ERSP measure in response to right pMFG(FPCN) or left aMFG (VAN) stimulation did not eliminate the relationships between within-VAN fMRI connectivity and the various VAN ERSP responses to right aMFG(VAN) spTMS (Wald χ^2's>6.4, p's<0.012). In particular, the alpha desynchronization effect at 400-600ms post-spTMS pulse shown in Figure 5d survived both of these analyses at Wald χ^2's>11.9, p's<0.0006.

In summary, using spTMS/EEG we discovered neural circuit influence signals that are associated with individual differences in resting-state within-VAN fMRI connectivity, and in a generalizable manner that was independent of clinical diagnosis. Specifically, we found that the lower the individual's level of within-VAN fMRI connectivity, the more prolonged was their EEG responses to spTMS stimulation of a right-sided VAN region – responses that involved profound below-baseline desynchronization centered on alpha-range frequencies.

Discussion

Here we have identified a biobehavioral phenotype within the broader clinical syndrome of PTSD, characterized by impairments in the delayed recall of verbal memory and resting-state fMRI connectivity of the VAN. This phenotype generalized across two independent and demographically/clinically distinct populations of patients and healthy individuals. It also powerfully moderated treatment outcome, despite being unrelated to current symptoms or comorbidities (hence clinically "latent"). Moreover, using concurrent spTMS/EEG to interrogate direct neurostimulation-evoked neural signal flow, we identified a neurophysiological circuit response that is associated with the degree of within-VAN fMRI connectivity. Specifically, we found that poorer within-VAN connectivity was reflected in a more prolonged circuit perturbation to single TMS pulses delivered to a right-sided anterior prefrontal VAN region, taking the form of profound alpha-range below-baseline desynchronization. From a clinical perspective, these findings help ground clinically-meaningful variation within the syndrome of PTSD in objective and quantifiable features. From a translational perspective, by identifying neurophysiological direct stimulation-evoked signal flow correlates for altered within-VAN fMRI connectivity we advance a basic understanding of on aspect of what, at least within-VAN, resting fMRI connectivity may index. Doing so thus also identifies a potential neurophysiological target for remediation through plasticity induction using repetitive TMS-based treatment targeting this region.

Network and behavioral mechanisms of PTSD

Prior neuroimaging and behavioral work has generally treated PTSD as a single clinical group, contrasting PTSD cases with healthy participants (though DSM-5 now recognizes a dissociative subtype)(*45*). This has resulted in substantial inconsistencies in the literature. In the case of the VAN, for example, various authors have argued for over-activity or over-connectivity of the VAN in PTSD, by virtue of its response to salient stimuli such as threat cues (*46, 47*). However, results regarding resting-state VAN connectivity have been inconsistent, with evidence of both increased (*48*) and decreased (*23, 49, 50*) within-VAN connectivity. It has also been noted that abnormalities associated with PTSD are typically greater when comparing patients to trauma-naïve healthy controls but diminished, or even absent, when comparing to well-matched trauma-exposed healthy controls (*51, 52*). Moreover, we are unaware of any prior report that applies the same analytical methods across two independent cohorts to determine whether a specific network connectivity finding generalizes across PTSD studies.

Our findings argue that these inconsistencies and lack of generalization across cohorts or studies may stem from failure to account for the biological heterogeneity within the syndrome of PTSD, as well as an uncontrolled differential sampling of the heterogeneity that occurs in each study. Rather, consistent mechanistically- and clinically-meaningful neurobiological phenotypes in PTSD cases can emerge by anchoring stratification of PTSD clinical populations on objectively quantifiable factors, e.g. verbal memory and within-VAN functional connectivity. Moreover, while

neurocognitive impairments have been frequently found in PTSD (*7*), with verbal memory representing one of the areas of greatest impairment, many PTSD patients nonetheless perform within the healthy range. Hence, we focused our analyses on a differentiation of PTSD cases who were impaired on verbal memory (defined as performing outside of a discriminant-determined healthy range), compared to those PTSD cases who performed similarly to controls, and would thus be expected to look similar to controls in terms of relevant fMRI connectivity patterns. It is also important to note that were we to solely use subjectively reported or clinician-rated symptoms to identify this biobehavioral phenotype, we would have failed, as it was not consistently associated with differences in symptom expression, even though it powerfully predicted subsequent treatment response. Thus, our findings are consistent with recent proposals to shift away from symptoms for defining disorders to a brain information processing-based approach (*53*).

Consistent with our findings, a role of the VAN in verbal memory is suggested by multiple prior findings. Neuroimaging meta-analysis of activation during performance of memory tasks has found that activity in the VAN is associated with increased familiarity of remembered items (*16*), as well as in memory of verbal over pictorial stimuli (*54*). Resting-state fMRI within-VAN connectivity has also been found to predict delayed recognition memory (*55*). Memory impairments observed as part of "cognitive aging" have also been associated with decreased within-VAN connectivity (*56, 57*), though other findings have also implicated aberrant connectivity across a broader set of brain networks in memory impairment (*17*).

We also note that while we found that verbal memory-impaired PTSD patients had lower within-VAN fMRI connectivity than both trauma-exposed controls and verbal memory-intact PTSD patients, impairments in memory and aberrant within-VAN connectivity are likely two related but independent measures of what is likely a core deficit in an underlying information processing capacity, and are thus not redundant. Indeed, an interaction between these two factors was critical for effectively predicting treatment outcome. While most individuals with poor delayed recall of verbal memory in Study 1 also showed reduced within-VAN fMRI connectivity and poor treatment outcome, there are some memory-impaired individuals with healthy-range within-VAN fMRI connectivity that display favorable treatment outcomes. There may therefore appear to be an inconsistency between our association of memory impairments with poor within-VAN connectivity and the necessity of utilizing both measures to predict treatment outcome (rather than just one, were they to contribute entirely redundant information). However, poor delayed recall of verbal memory may occur due to multiple reasons, not all of which are related to the within-VAN memory processes implicated here per se (e.g. distractibility, attention, fatigue etc). These other reasons may index unrelated circuitry characteristics. As memory tasks require the interaction of multiple cognitive networks(*16*), within-VAN connectivity may be impaired in some individuals but memory performance may remain intact. Likewise, factors related to variations in individual mental processes indexed during resting state, as well as simple measurement error, may result in lower within-VAN connectivity for reasons not related to their relationship to verbal memory. In other words, each measure contains statistical "noise" relating to multiple factors that do not index the core neurocircuitry deficit characterizing subtype treatment resistance. In this way, the treatment prediction

findings are, in fact, the most telling. Specifically, only in those individuals who have both poor memory and low within-VAN connectivity (i.e. in whom there is confluence of measures mapping the core deficit) is treatment ineffective, and not so for individuals in whom these measures may diverge in indexing the core deficit due to noise or variance from other factors.

Future work can build on these findings in several ways. We examined resting-state connectivity, but different relationships may emerge when looking at memory task-related fMRI connectivity. It may also be that a free recall-based verbal memory test may prove more sensitive to within-VAN connectivity abnormalities in PTSD as it suffers from less of an accuracy ceiling effect than the recognition-based recall task used in here. Moreover, given the role of the VAN in a range of cognitive operations (*58, 59*), other tasks that tap into these elements of VAN function may similarly be able to capture the phenotype we report here. It is also important to consider that every metric has its own test-retest-reliability, and even though verbal memory recall and fMRI connectivity both have relatively high levels of reliability, their covariation and treatment outcome prediction capacity is nonetheless gated by the reliability of each, as well as that of the outcome measure. Additional work is therefore necessary in refining which aspect(s) of verbal memory (or related constructs) and within-VAN resting fMRI connectivity are closely tied to one another in order to better understand this brain-behavior relationship. Finally, it will be important to test in future research whether both the relationship between within-VAN connectivity and verbal memory, and their joint relationship to treatment outcome, is specific to PTSD. As noted above, prior work has found associations between VAN functioning and memory unrelated to PTSD (*55-57*). There have also been implications of verbal memory alone in predicting outcome in disorders as diverse as bipolar disorder, psychosis and drug addiction(*60-63*), and we have found that disruptions in VAN are a feature common to many major psychiatric disorders (*64, 65*). Thus, we cautiously speculate that the VAN/memory relationship will generalize to other conditions and predict poor treatment outcome in other contexts.

Neurophysiological mechanisms of differences in within-VAN fMRI connectivity and implications for treatment

In this study, we sought to go beyond a correlative characterization of the biobehavioral phenotype discussed above, and identify potential neurophysiological mechanisms that may account for differences in within-VAN fMRI connectivity. To do this, we interrogated the concurrent EEG responses to single TMS pulse stimulation of bilateral VAN regions located in the anterior middle frontal gyrus, compared to a nearby posterior middle frontal region that is part of the FPCN. In prior concurrent spTMS/fMRI work, we found that stimulation of the same right VAN region, but not the right FPCN region, resulted in increased TMS-evoked within-VAN fMRI connectivity (*43*).

We now found that lower levels of within-VAN fMRI connectivity were associated with profound below-baseline alpha-range desynchronization for hundreds of milliseconds (~400-800ms) after the TMS pulse. This result is important for multiple reasons. First, since no prior work has investigated the association of response to spTMS/EEG with resting fMRI connectivity, these findings open a new window into understanding the neurophysiological meaning of differences in fMRI resting

connectivity. Second, we found this relationship after rigorous correction for multiple comparisons and in a generalizable manner that was independent of clinical state. As such, we anticipate that these findings will be of broad relevance to fMRI research. More generally, our spTMS/EEG results also provide a perspective on which elements of causal signal flow within a network may relate to within-VAN fMRI-measured network connectivity, and establish spTMS/EEG as a brain mapping tool for understanding the neural basis of resting state fMRI network measures when applied across other networks and stimulation sites.

One way to contextualize our findings is that normal levels of within-VAN resting-state fMRI connectivity (e.g. as typical of memory-intact patients or healthy controls) may make the VAN resilient to perturbation by a TMS pulse. In those individuals, the phase-locked response (i.e. TER) and oscillatory power changes (i.e. ERSP) largely return to baseline by ~400ms. By contrast, the same network may be more susceptible to perturbation by the TMS pulse in individuals with lower within-VAN connectivity (e.g. as typical of memory-impaired patients), wherein the oscillatory power changes continue for at least 800ms, which was the end of the EEG epoch we analyzed. Though presently unknown, it these results may carry implications for the effects that repeated TMS pulses, such as used in therapeutic repetitive TMS protocols, have on network neurophysiology across individuals with different levels of within-VAN fMRI connectivity. Individuals with low fMRI connectivity may, for example, demonstrate greater impact of the prior pulse on the next pulse by virtue of the prolonged period of alpha-range desynchronization from one pulse interacting with the next one.

Though still little is understood about the specific mechanisms associated with this late alpha-range desynchronization, it has been reported in motor cortex stimulation that it reflects a non-phase-locked aspect of the spTMS/EEG response and that it is sensitive to agonists of either the gamma-aminobutyric acid (GABA)-A or GABA-B receptors (*36*). In both cases, alpha desynchronization is increased by drugs that stimulate those receptors, suggesting that the increased and prolonged alpha-range desynchronization observed in individuals with lower within-VAN connectivity may index a larger inhibitory response to VAN spTMS stimulation. This interpretation contrasts with a common view of alpha-range oscillatory power in task and resting-state contexts, which argues that alpha reflects local inhibitory processing (*66*), and thus greater alpha desynchronization might actually mean less inhibition. However, the relationship between task and resting alpha oscillations and spTMS-induced late alpha desynchronization remains to be investigated. Likewise, future work should examine the relationship between VAN alpha power at rest and spTMS-induced late alpha desynchronization since altered alpha power has been observed in PTSD (*67*), and pre-spTMS alpha power has been found to predict aspects of the response to the spTMS pulse (*68*).

Identification of the right anterior middle frontal VAN node as a brain target at which stimulation evokes within-VAN fMRI connectivity-correlated EEG responses also carries potential clinical implications. Specifically, it suggests that this region may be a promising target for remediating the within-VAN fMRI connectivity deficit found in memory-impaired PTSD patients. This possibility is further supported not only by our prior spTMS/fMRI work (*43*), but also by a recent finding that examined the impact of high frequency repetitive TMS stimulation of either the right or left-sided anterior middle

frontal gyrus VAN regions (*69*). In that study, repetitive stimulation at 10Hz, which is thought to increase neuronal excitability (*34*), resulted in increased within-VAN resting-state fMRI connectivity, but only after stimulation of the right-sided VAN target. Though we do not know why the correlation with fMRI connectivity was lateralized to the right-sided VAN spTMS/EEG target in our study, our findings are nonetheless consistent with those of the 10Hz repetitive TMS study (including with respect to lateralization). Intriguingly, the vast majority of repetitive TMS treatment studies for PTSD have targeted a right-sided prefrontal region in the vicinity of our VAN region (*70-73*) and have found clinical efficacy. Likewise, disruptive and facilitating TMS manipulations of nearby right-sided prefrontal regions have been found to alter memory encoding or recall (*74, 75*). Most exciting is the potential that optimizing the TMS treatment for the patient could be guided by monitoring changes in spTMS/EEG responses to right anterior middle frontal VAN node stimulation, including as a function of baseline within-VAN connectivity.

Limitations

It is important to consider that while we identified consistent patterns of biological heterogeneity across two independent and clinically/demographically diverse samples, the treatment prediction findings need to be replicated and further developed for our treatment prediction finding to impact clinical care. Likewise, fMRI may be less well suited to ultimate clinical translation than EEG.

Conclusion

The shift from overly-broad symptom-based descriptive diagnostic approaches in psychiatry to mapping objectively-defined phenotypes and perturbing circuits for inferential power, as encouraged by our findings, holds great promise for deepening our understanding of the factors dictating clinical heterogeneity and variability in treatment response, uncovering mechanisms of illness, and establishing avenues for novel and personalized treatments. Moreover, the fact that an objectively-discriminated group of patients do not respond to standard evidence-based treatment for PTSD underscores the need to apply such an approach for the purposes of improving clinical decision-making and patient outcomes.

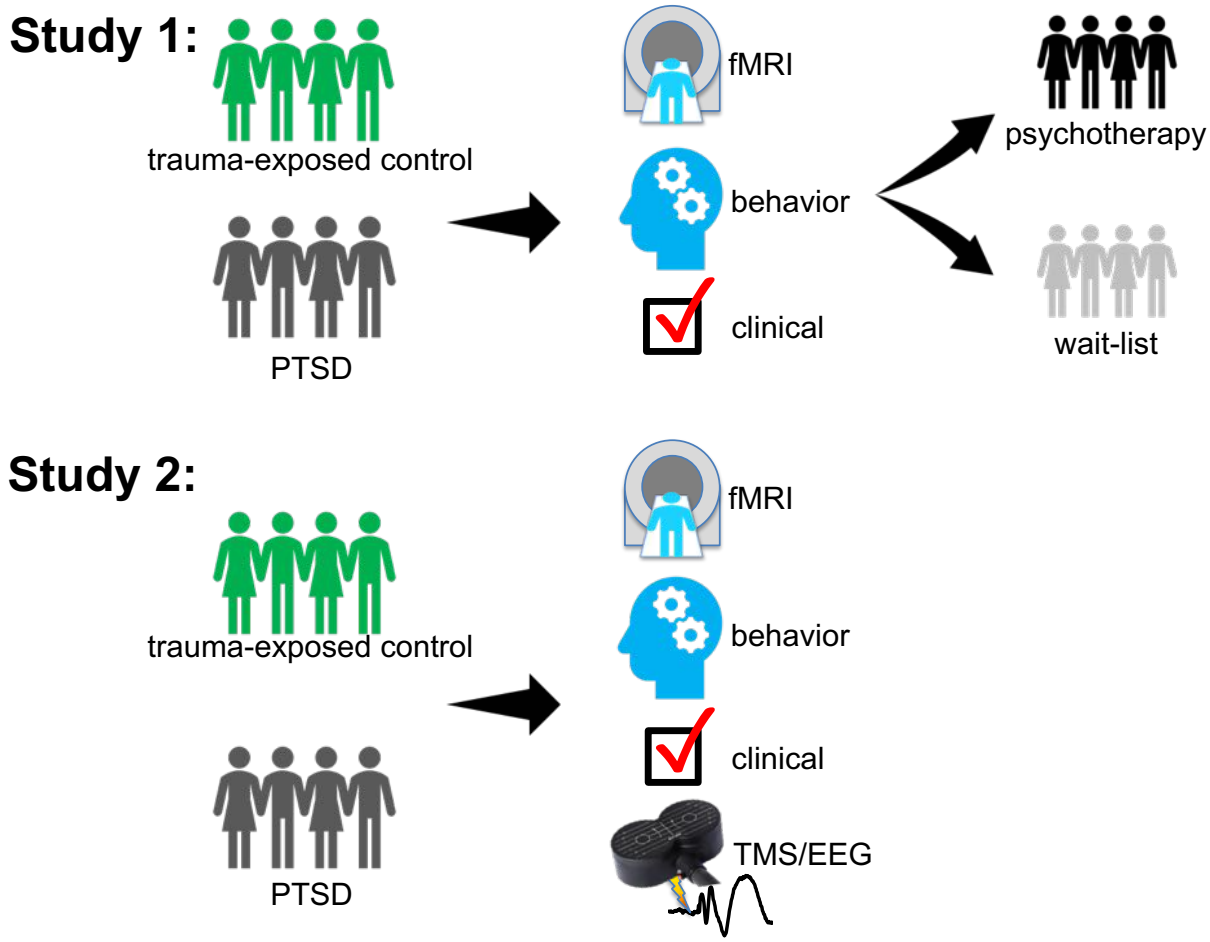

Figure 1: **Overview of the experimental design.**

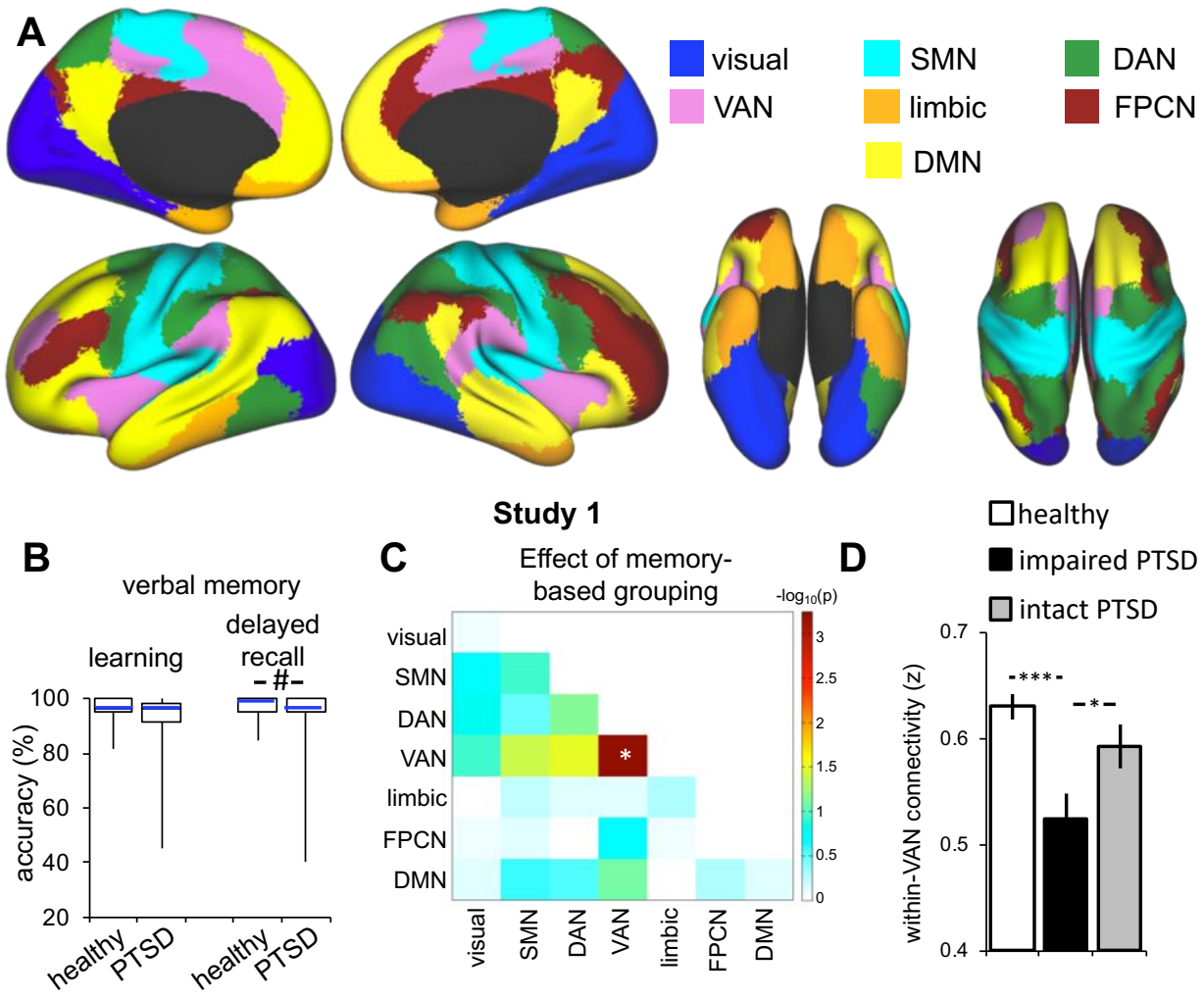

Figure 2: **Impairment in verbal memory delayed recall is associated with poor within-ventral attention network (VAN) resting-state fMRI connectivity in PTSD (Study 1).** (A) 3-D renderings of the seven previously-identified set of seven canonical cortical connectivity networks used for resting-state fMRI connectivity analyses (other abbreviations: SMN=somatomotor network, DAN=dorsal attention network, FPCN=frontoparietal network, DMN=default mode network). (B) Only blunted verbal learning delayed recall in PTSD cases survived FDR correction across the neurocognitive tests examined (Wald χ^2=6.0, p=0.014, p_{FDR}=0.0431). # FDR p<.05. (C) Results of the 3-level effect of group (healthy, impaired memory PTSD patients, intact memory PTSD patients) in generalized linear models predicting each network to network connectivity pair. The plot show $-\log_{10}$(p-value) of the effect of group term. Only within-VAN connectivity survived FDR correction (Wald χ^2=14.8, p=0.0006, p_{FDR}=0.015; white asterisk). (D) Bar graph showing the group effect on within-VAN connectivity, demonstrating impaired connectivity only in the impaired PTSD group, relative to both the healthy and intact PTSD groups. * p<.05, *** p<.001. Bar graphs show means and standard errors (for normally distributed variables), while box and whisker plots show medians, interquartile ranges, minima and maxima (for variables with skewed distributions).

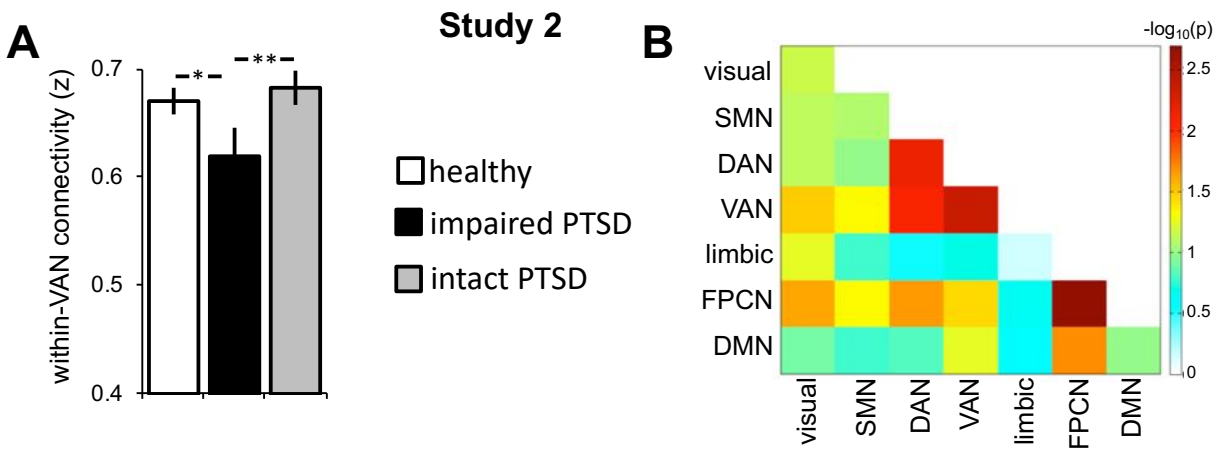

Figure 3: Generalization of the memory-related within-VAN fMRI connectivity impairment to an independent sample of patients and controls (Study 2). (A) Results of the 3-level effect of group using the same cutoffs and analytical approach as in Study 1. This demonstrates replication of the reduction in within-VAN fMRI connectivity only in the impaired memory PTSD group, relative to both the healthy and intact memory PTSD group (Wald χ^2=11.4, p=0.003). (B) The memory-related impairment in within-VAN fMRI connectivity also survived FDR correction across all network pairs (p_{FDR}=0.009). The plot show $-\log_{10}$(p-value) of the effect of group term. * p<.05, ** p<.01. Shown are means and standard errors.

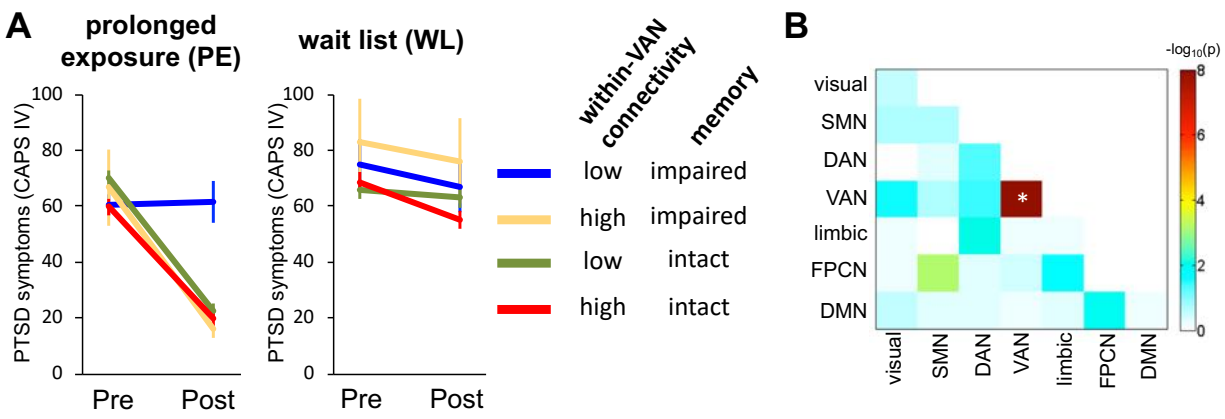

Figure 4: Poor treatment outcome for patients with impairments in memory and within-VAN connectivity (Study 1). Patients were randomized to a highly evidence-based psychotherapy treatment (prolonged exposure (PE)) or a wait list control (WL). (A) Generalized linear mixed models in an intent-to-treat analysis revealed a highly significant moderation effect (treatment group by memory by connectivity by time interaction). A median split on the fMRI connectivity variable is shown for illustrating the mixed model result (i.e. low/high connectivity). (B) Within-VAN connectivity likewise survived FDR correction across all network pairs in moderating treatment outcome ($p_{FDR}=10^{-7}$; white asterisk) based on the treatment group by memory by connectivity by time interactions term. The plot show $-\log_{10}$(p-value) of this term for each network pair.

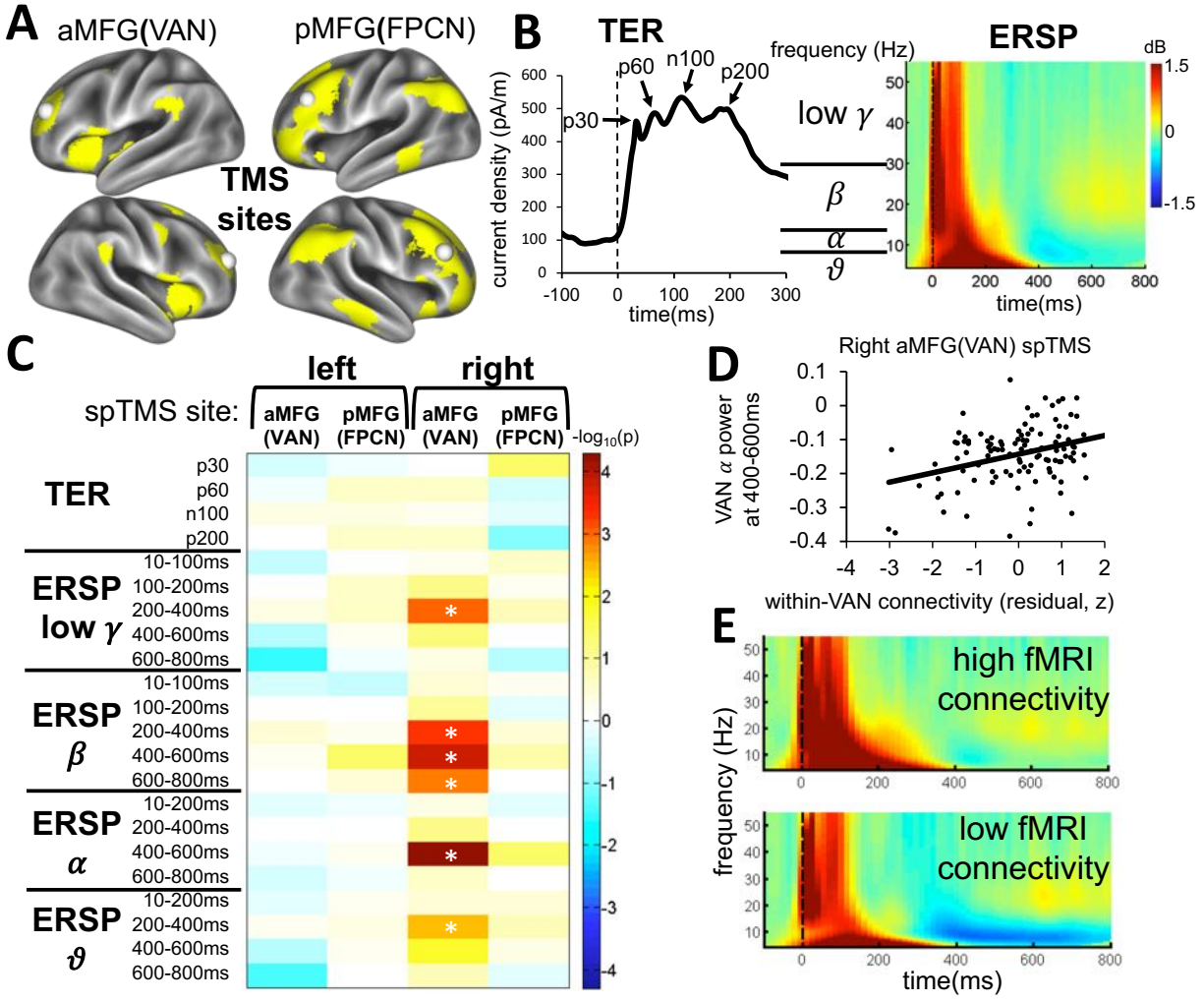

Figure 5: Relationship of within-VAN resting-state fMRI connectivity to neurophysiological causal circuit influence signals detected using concurrent spTMS/EEG. (A) TMS was delivered to one of two stimulation sites, bilaterally. These sites were identified based on independent components analyses on resting-state fMRI data from a separate cohort (yellow clusters). The TMS targets (white spheres) were either in the anterior middle frontal gyrus (aMFG, part of the VAN) or posterior middle frontal gyrus (pMFG, part of the FPCN). (B) Illustration of the spTMS/EEG signals quantified, which covered both TMS-evoked responses (TERs) and event-related spectral perturbations (ERSPs). See online methods for the TER time windows and ERSP frequency ranges. Dashed line indicates the timing of the TMS pulse. (C) A significance plot of the generalized linear models relating individual differences in within-VAN fMRI connectivity across all participants (healthy and PTSD) to individual differences in each EEG measure, for each of the stimulation sites. All EEG measures reflect an average of the denoted source-space signals across all vertices comprising the VAN, thus correlating within-VAN fMRI connectivity to the various EEG responses in the VAN to stimulation of various cortical sites. Only ERSP measures for right

aMFG(VAN) stimulation survived FDR correction (denoted by asterisks). The plot show $-\log_{10}(p)$ of the correlation of within-VAN fMRI connectivity with spTMS/EEG measures. (D) Scatter plot of one of the FDR-significant relationships, demonstrating that individuals with lower within-VAN fMRI connectivity had a more profound alpha-range desynchronization 400-600ms after the TMS pulse (i.e. below-baseline levels of alpha power). (E) ERSP plots for illustration of the significant findings. We averaged the ERSPs for participants in the top and bottom third of the within-VAN fMRI connectivity distribution in order to be able to visualize the correlation findings across the whole time-frequency range. This demonstrates the prolonged and profound alpha-range desynchronization from ~400 to ~800ms after the TMS pulse associated with reduced levels of within-VAN fMRI connectivity.

Materials and Methods

Methods are presented here in brief, with full details available in the supplemental materials.

Study Design

We report on data from two studies, including cross-sectional case-control data from both studies (involving healthy participants and those with PTSD), as well as longitudinal treatment outcome data from Study 1. Each study includes fMRI, behavioral, clinical and demographic measures, while Study 2 additionally includes spTMS/EEG data. The primary analyses are cross-sectional and focus on relating variation in cognitive task performance among PTSD patients (and with respect to healthy individuals) to variation in resting-state network connectivity. Additional cross-sectional analyses test how these brain-behavior relationships correlate with clinical symptoms, as well as the degree to which they can predict treatment outcome in a longitudinal analysis. Finally, we relate fMRI connectivity to spTMS/EEG-investigated directional neural signal flow in a subsequent cross-sectional analysis.

Participants and procedures

Figure 1 shows an overview of the experimental design. Study 1 included 112 primarily civilian participants (36 trauma-exposed healthy controls and 76 patients with PTSD), who underwent clinical, fMRI and behavioral assessments. Of these patients, 66 went on to a randomized controlled trial comparing prolonged exposure (PE) psychotherapy treatment to wait list. The PE protocol followed well-described procedures and was supervised by a leading expert in PE (B.O.R.). Study 2 included 245 Iraq/Afghanistan era combat veterans, with 117 being trauma-exposed healthy veterans and 128 having PTSD. They underwent the same assessments as Study 1 participants, as well as concurrent single pulse TMS/EEG probing of neural excitability to direct non-invasive stimulation. Study 2 participants did not get treatment.

The behavioral assessments were conducted through a computerized neurocognitive battery that probed verbal memory, attention, working memory and response inhibition. The fMRI consisted of an 8-minute resting-state fMRI scan, conducted either using spiral in-out imaging at Stanford (Study 1) or as a two-site study using echoplanar imaging at Stanford and New York University (Study 2). Stanford used a General Electric 750 3T Scanner, while New York University used a Siemens Skyra 3T scanner. Preprocessing and connectivity assessment followed conventional procedures.

The TMS/EEG assessment involved stimulation with single TMS pulses to several sites within the prefrontal cortex, localized to either the VAN or FPCN, while measuring concurrent EEG responses. Preprocessing was accomplished through an automated artifact rejection algorithm previously published by our group, and EEG source localization followed conventional procedures.

Statistical Analyses

All statistical analyses were conducted in SPSS software (IBM Corporation, New York) and primarily used generalized linear models, with the principle exception of the treatment outcome prediction analyses, which used generalized linear mixed models. All tests and post-hoc analyses were corrected for multiple comparisons, the details of which are described in the appropriate sections of the main text, using two-sided tests. A memory-based division of PTSD patients was established based on the cutoff in a discriminant analysis that compared performance of the healthy and PTSD groups on the verbal memory test. The same cutoff was used for all analyses in both Studies 1 and 2. Analysis of treatment outcome prediction in the randomized clinical trial followed an intent-to-treat framework that incorporated all randomized study participants in the analysis.

References

1. APA, *Diagnostic and statistical manual of mental disorders*. (American Psychiatric Press, Washington DC, ed. 4th, 1994).
2. APA, *Diagnostic and statistical manual of mental disorders*. (American Psychiatric Press, Washington DC, ed. 5th, 2013).
3. I. R. Galatzer-Levy, R. A. Bryant, 636,120 Ways to Have Posttraumatic Stress Disorder. *Perspectives on psychological science : a journal of the Association for Psychological Science* **8**, 651-662 (2013).
4. C. W. Hoge *et al.*, Unintended Consequences of Changing the Definition of Posttraumatic Stress Disorder in DSM-5: Critique and Call for Action. *JAMA Psychiatry* **73**, 750-752 (2016).
5. D. J. Stein *et al.*, DSM-5 and ICD-11 definitions of posttraumatic stress disorder: investigating "narrow" and "broad" approaches. *Depress Anxiety* **31**, 494-505 (2014).
6. R. Rosell, T. G. Bivona, N. Karachaliou, Genetics and biomarkers in personalisation of lung cancer treatment. *Lancet* **382**, 720-731 (2013).
7. J. C. Scott *et al.*, A quantitative meta-analysis of neurocognitive functioning in posttraumatic stress disorder. *Psychological bulletin* **141**, 105-140 (2015).
8. M. R. Milad *et al.*, Presence and acquired origin of reduced recall for fear extinction in PTSD: results of a twin study. *J Psychiatr Res* **42**, 515-520 (2008).
9. M. M. Rigoli, G. R. Silva, F. R. Oliveira, G. K. Pergher, C. H. Kristensen, The role of memory in posttraumatic stress disorder: implications for clinical practice. *Trends Psychiatry Psychother* **0**, 0 (2016).
10. A. Etkin, A. Gyurak, R. O'Hara, A neurobiological approach to the cognitive deficits of psychiatric disorders. *Dialogues Clin Neurosci* **15**, 419-429 (2013).
11. M. J. Nijdam, G. J. de Vries, B. P. Gersons, M. Olff, Response to psychotherapy for posttraumatic stress disorder: the role of pretreatment verbal memory performance. *J Clin Psychiatry* **76**, e1023-1028 (2015).
12. B. O. Rothbaum, M. Davis, Applying learning principles to the treatment of post-trauma reactions. *Annals of the New York Academy of Sciences* **1008**, 112-121 (2003).
13. R. L. Aupperle, A. J. Melrose, M. B. Stein, M. P. Paulus, Executive function and PTSD: disengaging from trauma. *Neuropharmacology* **62**, 686-694 (2012).
14. J. S. Siegel *et al.*, Disruptions of network connectivity predict impairment in multiple behavioral domains after stroke. *Proc Natl Acad Sci U S A* **113**, E4367-4376 (2016).
15. A. M. Schedlbauer, M. S. Copara, A. J. Watrous, A. D. Ekstrom, Multiple interacting brain areas underlie successful spatiotemporal memory retrieval in humans. *Sci Rep* **4**, 6431 (2014).
16. H. Kim, Dissociating the roles of the default-mode, dorsal, and ventral networks in episodic memory retrieval. *Neuroimage* **50**, 1648-1657 (2010).
17. M. Y. Chan, D. C. Park, N. K. Savalia, S. E. Petersen, G. S. Wig, Decreased segregation of brain systems across the healthy adult lifespan. *Proc Natl Acad Sci U S A* **111**, E4997-5006 (2014).

18. J. R. Cohen, M. D'Esposito, The Segregation and Integration of Distinct Brain Networks and Their Relationship to Cognition. *J Neurosci* **36**, 12083-12094 (2016).
19. K. A. Tsvetanov *et al.*, Extrinsic and Intrinsic Brain Network Connectivity Maintains Cognition across the Lifespan Despite Accelerated Decay of Regional Brain Activation. *J Neurosci* **36**, 3115-3126 (2016).
20. V. Menon, Large-scale brain networks and psychopathology: a unifying triple network model. *Trends Cogn Sci* **15**, 483-506 (2011).
21. R. L. Buckner, F. M. Krienen, B. T. Yeo, Opportunities and limitations of intrinsic functional connectivity MRI. *Nat Neurosci* **16**, 832-837 (2013).
22. A. C. Chen, A. Etkin, Hippocampal network connectivity and activation differentiates post-traumatic stress disorder from generalized anxiety disorder. *Neuropsychopharmacology* **38**, 1889-1898 (2013).
23. Y. Zhang *et al.*, Intranetwork and internetwork functional connectivity alterations in post-traumatic stress disorder. *J Affect Disord* **187**, 114-121 (2015).
24. A. MacNamara, J. DiGangi, K. L. Phan, Aberrant Spontaneous and Task-Dependent Functional Connections in the Anxious Brain. *Biol Psychiatry Cogn Neurosci Neuroimaging* **1**, 278-287 (2016).
25. C. J. Keller *et al.*, Intrinsic functional architecture predicts electrically evoked responses in the human brain. *Proc Natl Acad Sci U S A* **108**, 10308-10313 (2011).
26. A. Etkin, Addressing the Causality Gap in Human Psychiatric Neuroscience. *JAMA Psychiatry* **75**, 3-4 (2018).
27. M. Hallett *et al.*, Contribution of transcranial magnetic stimulation to assessment of brain connectivity and networks. *Clin Neurophysiol* **128**, 2125-2139 (2017).
28. A. Giovanni *et al.*, Oscillatory Activities in Neurological Disorders of Elderly: Biomarkers to Target for Neuromodulation. *Front Aging Neurosci* **9**, 189 (2017).
29. S. Bestmann, E. Feredoes, Combined neurostimulation and neuroimaging in cognitive neuroscience: past, present, and future. *Annals of the New York Academy of Sciences* **1296**, 11-30 (2013).
30. N. C. Rogasch, P. B. Fitzgerald, Assessing cortical network properties using TMS-EEG. *Hum Brain Mapp* **34**, 1652-1669 (2013).
31. W. Wu *et al.*, ARTIST: A fully automated artifact rejection algorithm for single-pulse TMS-EEG data. *Hum Brain Mapp*, (2018).
32. A. T. Hill, N. C. Rogasch, P. B. Fitzgerald, K. E. Hoy, TMS-EEG: A window into the neurophysiological effects of transcranial electrical stimulation in non-motor brain regions. *Neurosci Biobehav Rev* **64**, 175-184 (2016).
33. S. W. Chung, N. C. Rogasch, K. E. Hoy, P. B. Fitzgerald, Measuring Brain Stimulation Induced Changes in Cortical Properties Using TMS-EEG. *Brain Stimul* **8**, 1010-1020 (2015).
34. V. Kozyrev, U. T. Eysel, D. Jancke, Voltage-sensitive dye imaging of transcranial magnetic stimulation-induced intracortical dynamics. *Proc Natl Acad Sci U S A* **111**, 13553-13558 (2014).
35. I. Premoli *et al.*, TMS-EEG signatures of GABAergic neurotransmission in the human cortex. *J Neurosci* **34**, 5603-5612 (2014).

36. I. Premoli *et al.*, The impact of GABAergic drugs on TMS-induced brain oscillations in human motor cortex. *Neuroimage* **163**, 1-12 (2017).
37. A. Schaefer *et al.*, Local-Global Parcellation of the Human Cerebral Cortex from Intrinsic Functional Connectivity MRI. *Cereb Cortex*, 1-20 (2017).
38. B. T. Yeo *et al.*, The organization of the human cerebral cortex estimated by intrinsic functional connectivity. *J Neurophysiol* **106**, 1125-1165 (2011).
39. IOM, *Treatment of posttraumatic stress disorder: An assessment of the evidence*. (The National Academies Press, Washington, DC, 2008).
40. G. A. Fonzo *et al.*, PTSD Psychotherapy Outcome Predicted by Brain Activation During Emotional Reactivity and Regulation. *Am J Psychiatry* **174**, 1163-1174 (2017).
41. G. A. Fonzo *et al.*, Selective Effects of Psychotherapy on Frontopolar Cortical Function in PTSD. *Am J Psychiatry* **174**, 1175-1184 (2017).
42. F. W. Weathers, T. M. Keane, J. R. Davidson, Clinician-administered PTSD scale: a review of the first ten years of research. *Depress Anxiety* **13**, 132-156 (2001).
43. A. C. Chen *et al.*, Causal interactions between fronto-parietal central executive and default-mode networks in humans. *Proc Natl Acad Sci U S A* **110**, 19944-19949 (2013).
44. M. S. Hamalainen, R. J. Ilmoniemi, Interpreting magnetic fields of the brain: minimum norm estimates. *Med Biol Eng Comput* **32**, 35-42 (1994).
45. R. J. Fenster, L. A. M. Lebois, K. J. Ressler, J. Suh, Brain circuit dysfunction in post-traumatic stress disorder: from mouse to man. *Nature reviews. Neuroscience* **19**, 535-551 (2018).
46. I. Liberzon, J. L. Abelson, Context Processing and the Neurobiology of Post-Traumatic Stress Disorder. *Neuron* **92**, 14-30 (2016).
47. T. J. Akiki, C. L. Averill, C. G. Abdallah, A Network-Based Neurobiological Model of PTSD: Evidence From Structural and Functional Neuroimaging Studies. *Curr Psychiatry Rep* **19**, 81 (2017).
48. R. K. Sripada *et al.*, Neural dysregulation in posttraumatic stress disorder: evidence for disrupted equilibrium between salience and default mode brain networks. *Psychosom Med* **74**, 904-911 (2012).
49. Y. Zhang *et al.*, Disrupted resting-state insular subregions functional connectivity in post-traumatic stress disorder. *Medicine (Baltimore)* **95**, e4083 (2016).
50. Y. Liu *et al.*, Decreased Triple Network Connectivity in Patients with Recent Onset Post-Traumatic Stress Disorder after a Single Prolonged Trauma Exposure. *Sci Rep* **7**, 12625 (2017).
51. J. A. DiGangi *et al.*, Reduced default mode network connectivity following combat trauma. *Neurosci Lett* **615**, 37-43 (2016).
52. M. Kennis, A. R. Rademaker, S. J. van Rooij, R. S. Kahn, E. Geuze, Resting state functional connectivity of the anterior cingulate cortex in veterans with and without post-traumatic stress disorder. *Hum Brain Mapp* **36**, 99-109 (2015).
53. T. Insel *et al.*, Research domain criteria (RDoC): toward a new classification framework for research on mental disorders. *Am J Psychiatry* **167**, 748-751 (2010).

54. H. Kim, Differential neural activity in the recognition of old versus new events: an activation likelihood estimation meta-analysis. *Hum Brain Mapp* **34**, 814-836 (2013).
55. J. M. Andreano, A. Touroutoglou, B. C. Dickerson, L. F. Barrett, Resting connectivity between salience nodes predicts recognition memory. *Soc Cogn Affect Neurosci* **12**, 948-955 (2017).
56. V. La Corte *et al.*, Cognitive Decline and Reorganization of Functional Connectivity in Healthy Aging: The Pivotal Role of the Salience Network in the Prediction of Age and Cognitive Performances. *Front Aging Neurosci* **8**, 204 (2016).
57. F. W. Sun *et al.*, Youthful Brains in Older Adults: Preserved Neuroanatomy in the Default Mode and Salience Networks Contributes to Youthful Memory in Superaging. *J Neurosci* **36**, 9659-9668 (2016).
58. J. Downar, D. M. Blumberger, Z. J. Daskalakis, The Neural Crossroads of Psychiatric Illness: An Emerging Target for Brain Stimulation. *Trends Cogn Sci* **20**, 107-120 (2016).
59. V. Menon, L. Q. Uddin, Saliency, switching, attention and control: a network model of insula function. *Brain structure & function* **214**, 655-667 (2010).
60. E. Aharonovich *et al.*, Cognitive deficits predict low treatment retention in cocaine dependent patients. *Drug Alcohol Depend* **81**, 313-322 (2006).
61. A. Faerden *et al.*, Apathy, poor verbal memory and male gender predict lower psychosocial functioning one year after the first treatment of psychosis. *Psychiatry Res* **210**, 55-61 (2013).
62. T. Deckersbach *et al.*, Memory performance predicts response to psychotherapy for depression in bipolar disorder: A pilot randomized controlled trial with exploratory functional magnetic resonance imaging. *J Affect Disord* **229**, 342-350 (2018).
63. I. E. Bauer, M. Hautzinger, T. D. Meyer, Memory performance predicts recurrence of mania in bipolar disorder following psychotherapy: A preliminary study. *J Psychiatr Res* **84**, 207-213 (2017).
64. M. Goodkind *et al.*, Identification of a common neurobiological substrate for mental illness. *JAMA Psychiatry* **72**, 305-315 (2015).
65. L. M. McTeague *et al.*, Identification of Common Neural Circuit Disruptions in Cognitive Control Across Psychiatric Disorders. *Am J Psychiatry* **174**, 676-685 (2017).
66. W. Klimesch, P. Sauseng, S. Hanslmayr, EEG alpha oscillations: the inhibition-timing hypothesis. *Brain Res Rev* **53**, 63-88 (2007).
67. J. Dayan, G. Rauchs, B. Guillery-Girard, Rhythms dysregulation: A new perspective for understanding PTSD? *J Physiol Paris* **110**, 453-460 (2016).
68. V. Romei *et al.*, Spontaneous fluctuations in posterior alpha-band EEG activity reflect variability in excitability of human visual areas. *Cereb Cortex* **18**, 2010-2018 (2008).
69. R. S. Schluter, J. M. Jansen, R. J. van Holst, W. van den Brink, A. E. Goudriaan, Differential effects of left and right prefrontal high frequency rTMS on resting state fMRI in healthy individuals. *Brain Connect*, (2017).

70. M. T. Berlim, F. Van Den Eynde, Repetitive transcranial magnetic stimulation over the dorsolateral prefrontal cortex for treating posttraumatic stress disorder: an exploratory meta-analysis of randomized, double-blind and sham-controlled trials. *Can J Psychiatry* **59**, 487-496 (2014).
71. C. Clark, J. Cole, C. Winter, K. Williams, G. Grammer, A Review of Transcranial Magnetic Stimulation as a Treatment for Post-Traumatic Stress Disorder. *Curr Psychiatry Rep* **17**, 83 (2015).
72. P. S. Boggio *et al.*, Noninvasive brain stimulation with high-frequency and low-intensity repetitive transcranial magnetic stimulation treatment for posttraumatic stress disorder. *J Clin Psychiatry* **71**, 992-999 (2010).
73. H. Cohen *et al.*, Repetitive transcranial magnetic stimulation of the right dorsolateral prefrontal cortex in posttraumatic stress disorder: a double-blind, placebo-controlled study. *Am J Psychiatry* **161**, 515-524 (2004).
74. M. Sandrini, S. F. Cappa, S. Rossi, P. M. Rossini, C. Miniussi, The role of prefrontal cortex in verbal episodic memory: rTMS evidence. *J Cogn Neurosci* **15**, 855-861 (2003).
75. P. Turriziani, D. Smirni, M. Oliveri, C. Semenza, L. Cipolotti, The role of the prefrontal cortex in familiarity and recollection processes during verbal and non-verbal recognition memory: an rTMS study. *Neuroimage* **52**, 348-357 (2010).
76. D. D. Blake *et al.*, The development of a Clinician-Administered PTSD Scale. *J Trauma Stress* **8**, 75-90 (1995).
77. M. B. First, A practical prototypic system for psychiatric diagnosis: the ICD-11 Clinical Descriptions and Diagnostic Guidelines. *World Psychiatry* **11**, 24-25 (2012).
78. F. Weathers, B. Litz, D. Herman, J. Huska, T. Keane, paper presented at the The International Society For Traumatic Stress Studies, San Antonio, TX, 1993.
79. A. T. Beck, R. A. Steer, G. K. Brown, *Manual for Beck Depression Inventory-II*. (Psychological Corporation, San Antonio, TX, 1996).
80. E. B. Foa, E. A. Hembree, B. O. Rothbaum, *Prolonged exposure therapy for PTSD*. (Oxford University Press, New York, NY, ed. First, 2007).
81. S. M. Skevington, M. Lotfy, K. A. O'Connell, W. Group, The World Health Organization's WHOQOL-BREF quality of life assessment: psychometric properties and results of the international field trial. A report from the WHOQOL group. *Quality of life research : an international journal of quality of life aspects of treatment, care and rehabilitation* **13**, 299-310 (2004).
82. D. Wechsler, *Wechsler Abbreviated Scale of Intelligence.* . (The Psychological Corporation: Harcourt Brace & Company, New York, NY, 1999).
83. J. D. Corrigan, J. Bogner, Initial reliability and validity of the Ohio State University TBI Identification Method. *The Journal of head trauma rehabilitation* **22**, 318-329 (2007).
84. S. M. Silverstein *et al.*, Development and validation of a World-Wide-Web-based neurocognitive assessment battery: WebNeuro. *Behav Res Methods* **39**, 940-949 (2007).
85. R. H. Paul *et al.*, Preliminary validity of "integneuro": a new computerized battery of neurocognitive tests. *Int J Neurosci* **115**, 1549-1567 (2005).

86. A. Etkin *et al.*, A cognitive-emotional biomarker for predicting remission with antidepressant medications: a report from the iSPOT-D trial. *Neuropsychopharmacology* **40**, 1332-1342 (2015).
87. G. H. Glover, S. Lai, Self-navigated spiral fMRI: interleaved versus single-shot. *Magn Reson Med* **39**, 361-368 (1998).
88. D. H. Kim, E. Adalsteinsson, G. H. Glover, D. M. Spielman, Regularized higher-order in vivo shimming. *Magn Reson Med* **48**, 715-722 (2002).
89. G. H. Glover, T. Q. Li, D. Ress, Image-based method for retrospective correction of physiological motion effects in fMRI: RETROICOR. *Magn Reson Med* **44**, 162-167 (2000).
90. L. Friedman, G. H. Glover, Report on a multicenter fMRI quality assurance protocol. *J Magn Reson Imaging* **23**, 827-839 (2006).
91. G. H. Glover *et al.*, Function biomedical informatics research network recommendations for prospective multicenter functional MRI studies. *J Magn Reson Imaging* **36**, 39-54 (2012).
92. W. R. Shirer, S. Ryali, E. Rykhlevskaia, V. Menon, M. D. Greicius, Decoding subject-driven cognitive states with whole-brain connectivity patterns. *Cereb Cortex* **22**, 158-165 (2012).
93. F. Tadel, S. Baillet, J. C. Mosher, D. Pantazis, R. M. Leahy, Brainstorm: a user-friendly application for MEG/EEG analysis. *Comput Intell Neurosci* **2011**, 879716 (2011).
94. A. Gramfort, T. Papadopoulo, E. Olivi, M. Clerc, OpenMEEG: opensource software for quasistatic bioelectromagnetics. *Biomed Eng Online* **9**, 45 (2010).
95. B. Fischl, M. I. Sereno, A. M. Dale, Cortical surface-based analysis. II: Inflation, flattening, and a surface-based coordinate system. *Neuroimage* **9**, 195-207 (1999).

Acknowledgements
We are grateful to input on the manuscript from Lukas Pezawas, Alan Schatzberg, Colleen Mills-Finnerty, Manjari Narayan, Lisa McTeague, Neir Eshel and Ellie Beam.
Funding: This work was funded by R01 MH091860 from the National Institute of Mental Health (NIMH) to AE, a grant from the Steven A. and Alexandra M. Cohen Foundation to NYU School of Medicine (to CRM) and from Cohen Veterans Bioscience to AE, and funds from Ann and Peter Tarlton to AE. AE and RO were also funded by the Sierra-Pacific Mental Illness Research, Education and Clinical Center (MIRECC) at the Palo Alto VA. WW was also funded by the National Key Research and Development Plan of China under Grant 2017YFB1002505. GEF was supported by NIMH grant T32 MH019938 and the Office of Academic Affiliations, Advanced Fellowship Program in Mental Illness Research and Treatment, Department of Veterans Affairs. PEV was supported by the Medical Research Council (grant no. MR/K020706/1) and is a Fellow of MQ: Transforming Mental Health (MQF17_24).
Author contributions: AE conceived of the study, conducted the analyses, wrote the paper and provided funding. YVZ, KKP, ES, PL, RTT, AT, SZ, BG, RE, JC, IE, EW, RH, SM, KD, SB, FB, AG, JA, JN, DJO, SEL, DAA contributed to data acquisition. ADM, GAF, WW, JHu, BP, PEV, JR, MSG, CJK, JRC,A, NC, JHa, SF, BOR, CRM, ETB, ROH contributed to the data analysis and paper writing. CRM additionally provided funding.
Competing interests: E.T.B. is employed 50% by the University of Cambridge and 50% by GlaxoSmithKline (GSK); he holds stock in GSK. No other authors report study-relevant conflicts of interest. Unrelated to the work here, AE owns equity in Akili Interactive and Mindstrong Health, and has consulted for Brainsway. BOR has received research support from Transcept Pharmaceuticals, royalties from Oxford University Press, Guilford, APPI, and Emory University and received an advisory board payment from Genentech. AE and CM have a patent pending for the treatment prediction work reported here. J.R. holds stock in Siemens Healthcare AG.
Data and materials availability: Study 1 data is available from AE, while Study 2 data are available from AE and CM and are managed under a Data Use Agreement between Stanford and NYU.

List of Supplemental materials:

Supplemental Methods
Supplemental Results
Figure S1: Neurocognitive task performance in PTSD.
Figure S2: No relationship between the memory/connectivity-related phenotype and symptoms in PTSD patients (Studies 1 and 2).
Figure S3: CONSORT diagram for the Study 1 treatment component
Figure S4: No differential change in either within-VAN connectivity (a) or delayed recall of verbal memory (b) following treatment (i.e. PE versus WL).
Figure S5: Individual data points for verbal memory delayed recall, within-VAN fMRI connectivity and percent change in CAPS total scores with treatment in PE arm completers in Study 1.
Table S1: Demographic and clinical characteristics of participants with means and (standard deviations) for Studies 1 and 2.
Table S2: Trauma type details for Studies 1 and 2 (percent of PTSD participants endorsing a category for their index trauma).
Table S3: Demographic and clinical characteristics of participants by memory-based groupings.
Table S4: Demographic and clinical characteristics of participants with means and (standard deviations) for the intent-to-treat analysis of treatment outcome and its moderation by verbal memory impairment and within-VAN fMRI connectivity.
Table S5: Demographic and clinical characteristics of participants in Study 2 who did or did not undergo spTMS/EEG (pooling across healthy and PTSD groups).

SUPPLEMENTAL MATERIALS

Methods

Participants

Study 1

Study 1 included 112 right-handed subjects in the primary component of this study, including 76 patients with PTSD, and 36 trauma-exposed healthy subjects (demographics and clinical characteristics in Supplemental Tables 1-4). All participants were recruited and scanned at Stanford University after signing a Stanford institutional review board-approved informed consent form, in accordance with the ethical principles in the Declaration of Helsinki. Out of the 76 PTSD patients, 59 were unmedicated and thus were the focus of the primary analyses of cognition and fMRI connectivity. Furthermore, 66 of the 76 patients participated in a randomized clinical trial comparing prolonged exposure therapy to a wait-list control (clinicaltrials.gov identifier NCT01507948). Of these 66 patients, 51 were unmedicated and included amongst the 59 patients noted above, while 15 were on stable doses of an antidepressant (demographic and clinical characteristics in Supplemental Table 5).

Psychiatric diagnoses, or absence thereof for controls, were based on DSM-IV criteria using the Clinician-Administered PTSD Scale (CAPS) (*76*) for PTSD and the Structured Clinical Interview for the Diagnostic and Statistical Manual of Mental Disorders Axis I (SCID I) for other Axis I disorders (*77*). Participants were permitted to meet diagnostic criteria for comorbid mood and anxiety disorders secondary to PTSD. General exclusion criteria for both groups included the following: a history of psychotic, bipolar or substance dependence (within 3 months for patients and lifetime for controls), a history of a neurological disorder, greater than mild traumatic brain injury (i.e. >30 minutes loss of consciousness or >24 hour post-trauma amnesia), claustrophobia, and regular use of benzodiazepines, opiates, thyroid medications, or other CNS medication. Trauma-exposed healthy controls were required to have experienced a criterion A trauma, but not meet lifetime criteria for any Axis 1 psychiatric disorder, including PTSD.

Study 2

Study 2 involved 245 participants, including 128 with PTSD, and 117 trauma-exposed healthy participants (see Supplemental Tables 1-3). All participants were combat veterans serving during the Operation Iraqi Freedom (Iraq), Operation Enduring Freedom (Afghanistan) and Operation New Dawn periods. Participants were recruited and scanned at either Stanford University or New York University after signing an informed consent approved by the relevant University's institutional review board, in accordance with the ethical principles in the Declaration of Helsinki. Similar inclusion/exclusion and diagnostic criteria were used as above except that diagnoses were based on DSM-5(*2*) criteria

rather than DSM-IV(*1*). Participants were allowed to continue their current medications as long as the dose was stable for two months. 29% of the PTSD patients were taking a psychiatric medication (see Supplemental Table 1).

Treatment protocol (Study 1)

Treatment randomization and study flow

Following completion of baseline clinical assessments and fMRI scan, participants were randomized to one of two arms – treatment with prolonged exposure therapy, or a treatment waitlist – based on whether a number generated for each participant by a random number generator was odd or even. A total of 66 individuals were randomized 1:1 by study staff after completion of baseline clinical and neuroimaging assessments, with 36 being randomized to immediate treatment, and 30 to treatment waitlist (see CONSORT diagram, Figure S3; clinicaltrials.gov registration #NCT01507948). The duration of the clinical trial was from December 2010 through June 2015. The sample size was determined based on *a priori* power calculations to achieve significant differentiation in clinical outcome between exposure therapy and waitlist. Given the nature of the intervention and design, blinding of patients is not possible. If randomized to prolonged exposure, participants commenced treatment with a clinical psychologist trained to deliver prolonged exposure therapy. If randomized to treatment waitlist, individuals were instructed they would have a 10-week waiting period after which they would undergo a second clinical assessment and fMRI scanning session. After completion of this second assessment, individuals on treatment waitlist were then assigned to a study therapist for completion of prolonged exposure therapy (to ensure all participants received study treatment). However, treatment after wait-list was outside of the intent-to-treat randomization framework, and thus not analyzed here. There were no adverse events reported in the course of the study.

Treatment Frequency and Length

Treatment sessions occurred on either a once or twice-weekly basis, for a total of either 9 or 12 90-minute sessions. At sessions 2, 4, 6, and 8 individuals were administered the PTSD-Checklist Civilian Version for DSM-IV (*78*) as well as the Beck Depression Inventory-II (*79*) to track response to treatment. The benchmark used to establish adequacy of treatment response at Session 9 and subsequent termination was at least a 70% reduction in Session 8 PCL-C scores from the PCL-C total score at intake. If individuals met this benchmark, they were given the option to discontinue treatment after Session 9. If individuals did not meet this benchmark and/or wished to continue for an additional 3 sessions, treatment was terminated after Session 12. If treatment continued to 12 sessions, PCL and BDI measures were also administered at Sessions 10 and 12.

Therapist Competency and Supervision in Prolonged Exposure

All psychologists received training in delivery of prolonged exposure and were deemed to meet competence in delivery of the treatment by one of the treatment developers, consultant to the study, and clinician supervisor Barbara

Rothbaum, Ph.D. Dr. Rothbaum provided weekly group supervision to study therapists and reviewed video recordings of treatment sessions to rate compliance with the treatment protocol. Dr. Rothbaum watched the entirety of the first three treatment sessions for each therapist to ensure therapist familiarity and competence with all major components of the treatment (all delivered in the first three sessions), and she continued to review relevant portions of remaining sessions as directed by study therapists. All study therapists demonstrated good compliance with the therapy protocol and with no significant deviations, as demonstrated by good-to-excellent supervisor ratings of treatment session adherence.

Treatment Structure

Prolonged exposure therapy was delivered according to manualized procedures(*80*). All sessions were audio recorded on a digital voice recorder (entrusted to the patient to take home with them and for use in completing imaginal exposure homework assignments) as well as a digital video recorder (for the purposes of assessing treatment adherence, therapist competency, and clinical supervision). In brief, the structure and progression of treatment is as follows. Session 1 consisted of psychoeducation on posttraumatic stress disorder symptoms, the rationale for treatment, and treatment structure. It also involved additional assessment by the therapist of trauma history (including the index trauma, already established at intake), current symptoms, and current impairment. Breathing retraining was taught at the end of Session 1 and practiced collaboratively in session, which consisted of a normal inhalation and a controlled and slow exhalation with internal repetition of a calming word or phrase (e.g., “Calm”) and a pause between exhalation and next inhalation, which was audiotaped for the patient.

Session 2 consisted of homework review, self-report measures, a discussion of common reactions to trauma, a rationale for exposure as a treatment tool, construction of an exposure hierarchy for *in-vivo* exposure exercises, and selection of 2 to 3 hierarchy items for homework practice. Session 3 involved homework review, a brief rationale for imaginal exposure, and the first imaginal exposure in session for 45-60 minutes. This was followed by a processing portion in which the therapist and participant discussed the participant’s experience of the exposure, any insights received through that process, and areas to be further addressed in future exposures. Homework was then assigned (including completion of in-vivo exposures and imaginal exposures daily, and practice of breathing retraining). Session 4 consisted of the same format as Session 3.

Beginning in Session 5, the concept of trauma memory “hotspots” was discussed with participants, which were points in the memory during which the participant expressed the highest level of distress. The in-session imaginal exposure began to shift towards emphasizing hotspots in the memory in Session 5, at earliest, and sometimes Session 6 if agreed to be clinically appropriate by the participant and therapist. Session 6, 7, and 8 involved a similar format, with homework review, imaginal exposure to “hot spots”, processing, and homework

assignment. For participants reaching the PCL clinical benchmark in Session 8, and agreeing to end in 9 sessions, Session 9 consisted of homework review, a brief imaginal exposure of the entire trauma memory conducted in-session (20-30 minutes), a brief processing, and a final review of treatment progress and skills acquired. For participants not reaching the clinical benchmark and/or wishing to continue for an additional 3 sessions, Sessions 9-11 maintained the same format as Sessions 4-8. In this case, Session 12 served as the final session (which assumed the aforementioned format).

Post-Treatment Clinical Assessment

Approximately 4 weeks following the final treatment session, participants were invited to return to complete a post-treatment clinical assessment. A 4-week period was chosen to intercede between final session and post-treatment assessment in order to allow treatment changes to consolidate and symptom levels to equilibrate. Participants were administered the CAPS and SCID again at post-treatment to assess change in PTSD symptoms and comorbid diagnoses.

Clinical and behavioral assessments

Questionnaires and clinical scales

In addition to quantification of PTSD symptoms using the CAPS (for DSM-IV in Study 1 and DSM-5 in Study 2) and assessment of comorbid diagnoses using the SCID, participants across all studies also completed several self-report questionnaires. This included quality of life using the World Health Organization's WHOQOL-BREF survey (*81*), and depression using the Beck Depression Inventory II (*79*). Intelligence quotient (IQ) was estimated in both studies using the Wechsler Abbreviated Scale of Intelligence (WASI)(*82*). TBI was diagnosed in Study 2 based on loss of consciousness(*83*).

Neurocognitive test battery

We administered the same standardized computer-based neurocognitive test battery (*84, 85*) to participants in both studies, and which we had previously used in research on depression (*86*). The following cognitive tasks (and domains) were assessed:

Word list learning task (verbal memory): Participants are presented visually with 20 English words per learning block, one at a time, which they are asked to memorize. Words are closely matched on concreteness, number of letters and frequency. Each block ended with a test of immediate recall, which was done by presenting 20 sets of 3 words, only one of which was previously presented (which participants are asked to indicate). Learning occurred and was tested over three repetitions of the word list learning and immediate recall test blocks, with word combinations altered across the retention tests for each block. A delayed recall test is done 15 minutes later with another 20 sets of 3 words. Behavioral analyses were conducted on accuracy.

Continuous performance task (sustained attention): Participants view a series of letters (D, C, G or T) and indicate when the current letter is the same as one letter prior (display time 200ms, ISI 2600ms). There are 63 stimuli in total, with 12 trials in which the current letter is the same as the prior letter. Behavioral analyses were conducted on accuracy and correct trial reaction time.

Digit span forward task (working memory): Participants are presented visually with series of digits of varying lengths, and asked to enter those digits in the order in which they were presented. The first trial includes 3 digits, and two trials are presented at the same length level, followed by a progressive increasing of the digit span length across trials. The task ends after 2 incorrect trials at the same length level, or when the maximum 9-digit length is reached. Behavioral analyses were conducted on the maximum recall span.

Color-word Stroop interference task (inhibitory control): Participants complete two conditions, one in which they indicate they indicate the name of color words (ignoring font color), and another where they indicate the color that the word was presented in (ignoring the word). In each trial, there are one of four different color words (red, blue, yellow, green), displayed in one of four colors (red, blue, yellow, green), with four buttons displayed underneath for the participant's response (one for each color word, all in black font). Stroop interference is calculated on correct trial reaction times by subtracting word naming from color naming.

Go/NoGo task (response inhibition): Participants see the word 'PRESS' appear repeatedly on the screen (display time 500ms, ISI 500ms). Green presentations (126 trials) indicate that participants should press the space bar as quickly as they can, while for red presentations (42 trials) participants are to withhold their response. Behavioral analyses were conducted on accuracy and correct trial reaction times.

Trails B task (flexibility): Participants are asked to connect a series of 13 digits (1 to 13) and 12 letters (A to L) in alternating digit/letter sequence (1-A-2-B, etc) using their mouse. Correct responses are accompanied by a line appearing between the last and current choices. Behavioral analyses are conducted on accuracy and average connection times between letters/numbers.

Choice reaction time task (processing speed): Participants indicate with arrow keys which of two black circles turned green on the screen. The green circle stays green until the correct response is made. There are 20 pseudo-randomly presented trials, with a 2-4 second jittered inter trial interval. Behavioral analyses are conducted on correct trial reaction times.

MRI data acquisition and preprocessing

General scan parameters.

All resting-state fMRI scans were eight minutes in length. Imaging for the participants in Study 1 was performed on a 3T General Electric 750 scanner at Stanford University. Participants in Study 2 were scanned either on the Stanford GE 750 scanner or at NYU on a Siemens 3T Skyra scanner.

For Study 1, 29 axial slices (4-mm slice thickness) were acquired covering the whole brain, using a T2- weighted gradient-echo spiral-pulse sequence (repetition time, 2000 ms; echo time, 30 ms; flip angle, 80 degrees; slice spacing, 0.5; field of view, 22cm; matrix size, 64x64) (*87*). An automated high-order shimming method based on spiral acquisitions was used before acquiring fMRI scans (*88*) in order to reduce blurring and signal loss arising from field inhomogeneities. In addition, for retrospective correction of physiological motion effects in fMRI, RETROICOR was used (*89*). A high-resolution T1-weighted structural scan was acquired as follows: three-dimensional inversion recovery spoiled gradient-recalled acquisition in the coronal place with the following parameters: inversion time = 300 ms, TR = 8 ms, TE = 3.6 ms, flip angle = 15°, field of view = 22 cm, 124 slices, matrix = 256x192, acquired resolution = 1.5 x 0.9 x 1.1 mm. For Study 2, both sites acquired 32 axial slices with 3.5mm thickness using an echo-planar gradient-echo T2-weighted pulse sequence (repetition time, 2000ms; echo time, 29 ms; flip angle, 90 degrees; slice spacing, 0; field of view, 20cm; matrix size, 64x64). A high-resolution T1-weighted structural scan was acquired as follows: three-dimensional MPRAGE in the sagittal place with the following parameters: inversion time = 450 ms, TR = 8.21 ms, TE = 3.22 ms, flip angle = 15°, field of view = 24 cm, 184 slices, matrix = 256x256, acquired resolution = 0.9375 x 0.9375 x 1.0 mm. For both Studies 1 and 2, the quality of fMRI scans was monitored by MRI center staff weekly with scans of an Functional Biomedical Informatics Research Network (fBIRN) agar phantom, as previously described (*90, 91*).

For Study 2, as it was a two-site MRI study, prior to study initiation, we harmonized image acquisition sequences across the two scanners. This involved both assessing image quality and signal to noise ratio (SNR) of images acquired using different parameters at each site, as well as acquisition of the same sequences on several traveling non-study control participants. Scanning of traveling non-study controls was repeated at roughly mid-study. Though the same acquisition sequences were used at both sites, differences between scanners are expected. For example, the echo-planar resting-state scans typically had more ventral prefrontal and temporal lobe susceptibility-artifact dropout at the Stanford site than the NYU site. The slice-based SNR was also significantly higher at NYU than at Stanford (mean (SD) for NYU: 235 (78) and Stanford: 194 (51); Wald χ^2=17.2, p= 0.00003). These differences in acquisition site were accounted for using a site variable in all statistical models for Study 2.

During the progress of the study, assessment of signal quality and stability was done as follows. For each scan, quality was assessed by quantitative and qualitative factors, with results regularly reported to MRI center staff and principle investigators at weekly meetings. Quantitative factors include: scan parameters (check for correctness), slice-based signal to noise ratio, and total root mean square head motion as well as framewise displacement. We also monitored

scanner performance by tracking reference voltage, imaging frequency, and bias field correction over time. Reference voltage (aka RF transmit reference voltage) determines the amplitude of the RF pulses. Imaging frequency variations can indicate scanner problems. The scanner's central frequency is typically set to the resonance frequency of water photons. Measurements of this are proportional to the field strength, and imaging frequency is a common calibration parameter and can be found in every image's DICOM header. Variations that exceed reference values can indicate magnet drift or RF instability. Qualitative factors were assessed visually by a trained image quality assessor. These included field of view clipping, wrapping, dropout, ringing/ striping, blurring, ghosting, RF problems (noise, spikes, leakage), and inhomogeneity.

Preprocessing

The first 5 acquired volumes (10 seconds) were dropped, the data were then motion corrected using FSL's mcFLIRT (http://fsl.fmrib.ox.ac.uk/fsl/fslwiki/MCFLIRT). The non-linear registration to standard space was performed using FSL's FNIRT, registration from functional to T1-weighted structural images was estimated using FSL's implementation of boundary-based registration (fsl.fmrib.ox.ac.uk/fsl/fslwiki/FLIRT_BBR). The mean white matter (WM) and cerebral spinal fluid (CSF) signal was estimated from the time-series using an MNI space defined WM/CSF mask transformed to the native functional space. The functional time-series was residualized with respect to the estimated WM/CSF signal. The data were then spatially smoothed with full-width half-maximum (FWHM) Gaussian of 6mm, consistent with our prior work and how our connectivity atlas was previously used (*92*). The data were residualized with respect to six motion parameters (estimated from mcFLIRT) to further account for motion effects. Next, volumes with framewise-displacement of >0.5 mm were removed from the data to further reduce motion-related artifact. Lastly, a bandpass filter was applied to data using cut-off frequencies of 0.008Hz – 0.1Hz. Only subjects with maximum root mean square motion <3mm were included in analyses.

fMRI connectivity analyses

A set of 100 regions of interest (ROIs) were defined based on a recently-published cortical parcellation derived from applying a combination of local gradient analysis and global signal similarity on an independent resting-state fMRI cohort (*37*). ROIs were mapped to seven previously identified functional networks (see Figure 2a) based on the spatial overlap between each ROI and each network (*38*). Connectivity strength was estimated using Pearson's correlation coefficient between the mean signals from each pair of *a priori* ROIs, which were then converted to z-scores using Fisher's r-to-z transformation. To further reduce data dimensionality in a meaningful way, we next used these values to calculate for each network the average within-network connectivity value as well as a pairwise between-network connectivity value for each pair of networks. This resulted in a set of 28 connectivity strength values representing

the within- and between-network resting-state connectivity profile for each subject.

spTMS/EEG data acquisition and preprocessing

Data acquisition

Anatomical targets for spTMS stimulation were determined based on an independent components analysis (ICA) of resting fMRI data from a separate group of individuals (*43*). These targets were then transformed to individual subject native space using non-linear spatial normalization with FSL (https://fsl.fmrib.ox.ac.uk/fsl/fslwiki) and used for TMS targeting. The targets were placed on each participant's T1-weighted anatomical MRI for neuronavigation using the Visor2 LT 3D neuronavigation system (ANT Neuro, Netherlands). Each of four target sites were stimulated with 60 pulses (biphasic TMS pulses, 120% of resting motor threshold), interleaved at a random interval of 3 ± 0.3 seconds using a MCF-B65 butterfly coil and a MagPro R30 TMS stimulator (MagVenture, Denmark). TMS sites included the FPCN and VAN nodes within the middle frontal gyrus bilaterally, as previously described (*43*), with targets identified for both the left and right hemispheres. For the stimulation, the TMS coil was placed tangentially to the scalp with the handle pointing backwards and laterally at an angle of 45° to the sagittal plane. Participants were instructed to relax and to fixate at a cross located on the opposing wall during each stimulation.

64-channel EEG data were recorded using two 32-channel TMS-compatible BrainAmp DC amplifiers and the Easy EEG cap with extra flat, freely rotatable electrodes designed specifically for TMS applications (BrainProducts GmbH, Germany). Electrode impedances were kept below 5 kOhms. EEG data were sampled at 5 kHz and an electrode attached to the tip of the nose was used as the reference. The electrodes were digitized relative to the scalp at the end of the spTMS-EEG session using the neuronavigation system. To avoid the artifact introduced by the coil recharge, the recharge time was delayed by 1500 ms.

Preprocessing, source localization and signal extraction

The spTMS/EEG data were cleaned and analyzed using custom MATLAB (Mathworks, Natick, MA) scripts. Specifically, a fully automated artifact rejection algorithm that we developed recently was employed to clean the spTMS/EEG data (*31*): 1) The initial 10 ms data segment following TMS pulses were discarded to remove the large stimulation-induced electric artifact. 2) The EEG data were downsampled to 1 kHz. 3) Big decay artifacts were automatically removed using ICA based on thresholding. 4) The 60 Hz AC line noise artifact was removed by a notch filter. 5) Non-physiological slow drifts in the EEG recordings were removed using a 0.01 Hz high-pass filter, and high-frequency noise was removed by using a 100 Hz low-pass filter. 6) The spectrally filtered EEG data was then re-referenced to the common average and epoched with respect to the TMS pulse (-500 ~ 1500 ms). 7) Bad trials were rejected by thresholding the magnitude of each trial. Bad channels were rejected based on the spatial correlations among channels. The rejected bad channels were then

interpolated from the EEG of adjacent channels. 8) Remaining artifacts were automatically removed using ICA. ICs related to the scalp muscle artifact, ocular artifact, ECG artifact, were rejected using a pattern classifier trained on expert-labeled ICs from other TMS/EEG data sets.

Source localization was performed using the Brainstorm toolbox (*93*). A three-layer boundary element model of the head was computed with the OpenMEEG plugin (*94*) based on FreeSurfer average brain template (*95*). A total of 3,003 rotating dipoles were generated on the cortical surface. The lead-field matrix was obtained by projecting the standard electrode positions onto the scalp. The current density of each dipole was then estimated by the minimum norm estimation approach (*44*) with depth weighting and regularization.

The source-space TMS-evoked response (TER) is defined as the average of the 3-D current density across trials and represents the phase-locked response to TMS. The event-related spectral perturbation (ERSP) is defined as the average of the log-time-frequency power maps of the 3-D current density across trials, with baseline correction (*95*). ERSP is suited for examining the induced oscillations that are not phase-locked to TMS. For each subject and stimulation site, the vertex-wise TER was computed by taking the norm of the TERs of all three orientations at each vertex. The network TER was then obtained by averaging the vertex-wise TER across all the vertices within the network, and assessed for the following time windows by averaging within each: p30 (25-35ms), p60 (45-70ms), n100 (100-150ms), p200 (175-225ms). Similarly, for each subject and stimulation site, the vertex-wise ERSP was computed by averaging the ERSPs of all three orientations at each vertex. The network ERSP was then obtained by averaging the vertex-wise ERSP across all the vertices within the network, and assessed for the following frequency bands: θ (4-7Hz), α (8-12Hz), β (13-30Hz), γ (31-50Hz), and time windows: 10-100ms, 100-200ms, 200-400ms, 400-600ms, 600-800ms. For each stimulation site, participants whose average TER is beyond the 4 standard deviations from the mean TER across all participants were excluded from the group analysis to ensure only high quality spTMS/EEG data were analyzed.

Statistical analyses

All statistical analyses were conducted in SPSS software (IBM Corporation, New York). Unless stated otherwise, cross-sectional effects of categorical or continuous variables were assessed using generalized linear models (GLM). For each test, the data met the assumptions of the test reported, with appropriate variances between groups for the test (with variances summarized as either error bars in plots or standard deviations in tables). Post-hoc tests of significant effects were conducted using Sidak correction for multiple comparisons on a significant GLM result. Each of the GLMs included a core set of covariates. For Study 1, this included core covariates for age, gender, education and head motion (as all participants were right-handed and the primary analyses used only medication-free patients). For Study 2, the core covariates included age, gender, education, head motion, site, handedness, and each of the

medication classes noted in Supplemental Table 1. Additional covariates in follow-up analyses are noted in the text for each of the studies. Correction for multiple comparisons was done using the false discovery rate (FDR), with each instance of FDR correction noted in the main text.

The memory-based grouping of PTSD patients (i.e. impaired vs intact) was done in SPSS for Study 1 by entering the delayed verbal memory recall accuracy scores for patients and healthy controls into a discriminant analysis in order to determine the optimal cut-point that discriminates the two groups. This revealed that 90% accuracy (or below) was optimal for identifying patients. We therefore binarized patients into an intact memory group (ie >90% accuracy, thus performing within the healthy range) and an impaired memory group (≤90% accuracy, thus performing outside the healthy range). The same cutoff was subsequently applied to Study 2 in order to maintain the same definition of the impaired and intact groups. Binarization was done so that the neural correlates of memory-related impairments in patients could be examined with respect to both unimpaired patients and healthy individuals.

For the treatment moderation analyses in the Study 1 treatment sample, we conducted intent-to-treat analyses using generalized linear mixed models (GLMM) with a robust estimator, to control for potential violations of model assumptions, implemented with a random intercept and fixed slope. This allowed us to include all participants who were randomized to PE or WL in the study, without the biases that may come from the typical completer studies conducted in neuroimaging studies. This also allowed us to examine moderator interactions with treatment-related change in symptoms while controlling for baseline symptom levels. The main GLMMs included factors for arm (PE vs WL), time (pre vs post), as well as within-VAN fMRI connectivity and/or the binarized verbal memory impairment variable defined above. The following effects were specified in the combined verbal memory/within-VAN connectivity moderation model in order to account for all lower-order interactions that might influence the higher-order four-way interaction effect of interest: time, group x time, verbal memory, fMRI connectivity, fMRI connectivity x verbal memory, time x verbal memory, time x fMRI connectivity, time x fMRI connectivity x verbal memory, group x time x verbal memory, group x time x fMRI connectivity, and group x time x verbal memory x fMRI connectivity. The F statistic corresponding to this latter 4-way interaction was used to assess a conjoint moderation effect of verbal memory and network efficiency on differential symptom change by treatment group. GLMMs examining only the moderating effects of memory or fMRI connectivity excluded the terms that include the variable no longer in the model. As these single moderator models reflect effects within the two interacting moderator model, we compared the memory/fMRI connectivity model to the single variable models using likelihood ratio tests to determine if the two moderator model explained significantly more variance in PE-related treatment outcome. Treatment-related changes in symptoms, memory and fMRI connectivity also used the same GLMM (including a random intercept and fixed slope), but included only terms for group and group x time interactions.

Results

Memory performance of the memory-defined groups in Studies 1 and 2

In Study 1, the median recall accuracy of the verbal memory-impaired PTSD subgroup was 82.5% (mean: 75%), indicating a notable performance impairment relative to the memory-intact PTSD subgroup (median/mean of 100%/98%) and the healthy group (median/mean 100%/97%). In Study 2, the median recall accuracy of the verbal memory-impaired PTSD subgroup was 85% (mean: 78%), indicating a notable performance decrement relative to the memory-intact PTSD subgroup (median/mean of 100%/98%) and the healthy group (median/mean 98%/96%).

Mapping brain to behavioral deficits in PTSD: investigating effects of potential confounding factors

Study 1

Amongst the three, verbal memory-based groups in Study 1, we found that age differed significantly, such that the impaired PTSD group was significantly older than both the healthy and intact PTSD groups (supplemental table 3; Wald χ^2=7.4, p=0.025; post-hoc pairwise impaired vs. healthy p=0.01, impaired vs. intact p=0.01). In addition to including age as a covariate in the analysis above, we verified in two additional ways that age was not the driving factor for the within-VAN connectivity differences we observed. First, amongst PTSD patients, we found that age itself was not significantly related to within-VAN connectivity (Wald χ^2=0.9, p=0.34). Second, we noted that the group differences in age were driven by the impaired PTSD group having several more individuals >55 years old (our study inclusion maximum age cutoff was 60). Thus, we tested the effect of excluding all participants >55 years old, and again found significantly lower within-VAN connectivity in the impaired PTSD group relative to each of the other groups using the same generalized linear model as above (Wald χ^2=10.2, p=0.006), but now observed no group differences in age (Wald χ^2=3.6, p=0.16). Finally, we tested whether the same brain-behavior relationship could be observed when including the medicated PTSD participants in Study 1, and again found that within-VAN connectivity was selectively lower in the verbal memory impaired PTSD patients compared to either healthy individuals or verbal memory intact PTSD patients (Wald χ^2=13.8, p=0.001). Similar results were obtained including only Study 1 patients who went on to take part in the randomized clinical trial described further below (Wald χ^2=14.8, p=0.0006).

Robustness of the identified relationship between verbal memory and within-VAN connectivity was further examined by repeating the test while controlling for general intelligence, as well as other cognitive measures. The memory-based grouping results held while controlling for general intelligence, in addition to the covariates noted above (Wald χ^2=20.2, p=0.00004). Likewise, the results held even after controlling for performance on other cognitive tests that

showed trend-level group differences in Figure S1, such as sustained attention accuracy and reaction times (Wald χ^2=20.3, p=0.00004), information processing speed reaction times (Wald χ^2=13.5, p=0.001), and working memory digit spans (Wald χ^2=14, p=0.0009). Within-VAN functional connectivity amongst patients also did not correlate with scores on these cognitive tests (Wald χ^2<1.9, p>0.19). We also considered the possibility that connectivity differences within the VAN reflected more basic/focal aspects of the signal fluctuation in VAN regions. Thus, we quantified the coefficient of variation within VAN regions, but did not find a significant effect of memory-based grouping on this measure (Wald χ^2=2.9, p=0.23).

Study 2

Beyond these large differences in samples noted in the main text, Study 2 PTSD patients were also significantly younger and had lower general intelligence than Study 1 PTSD patients (Wald χ^2's>6.0, p's<0.015), although healthy individuals did not differ on either measure across studies (Wald χ^2's<1.4, p's>0.23). Notably, demographic factors did not significantly differ between PTSD cases and healthy individuals in Study 2 nor did these differ in Study 2 when using the verbal memory-based grouping defined above (see Supplemental Tables 1 and 3). Critically, there were also no significant differences in age between the memory-based groups either (Wald χ^2=1.9, p=0.39).

As in Study 1, similar results were found in Study 2 using our memory-based grouping when controlling for general intelligence (Wald χ^2=10.1, p=0.006), sustained attention accuracy and reaction times (Wald χ^2=12.1, p=0.002), information processing speed reaction times (Wald χ^2=11.7, p=0.006), and working memory digit spans (Wald χ^2=10.9, p=0.004). As in Study 1, we also did not find a significant effect of the verbal memory-based grouping on VAN coefficient of variation (Wald χ^2=4.1, p=0.13).

Determining the clinical significance of impaired verbal memory and poor within-VAN connectivity: current symptoms and comorbidities

We next asked whether clinical aspects of PTSD, or its common comorbidities, differed in patients as a function of verbal memory delayed recall, within-VAN connectivity or their interaction. These analyses first focused on general symptom measures that had been assessed in both Studies 1 and 2. As seen in Supplemental Figures 3a and 3b, we found no effect of memory, within-VAN connectivity or their interaction on overall PTSD severity, as assessed by the Clinician-Administered PTSD Scales (CAPS) for DSM-IV or DSM-5 in Studies 1 or 2, respectively (Wald χ^2's<1.7, p>0.19). Repeating these analyses for CAPS subscales (three for Study 1 and four for Study 2), or CAPS dissociation items, failed to yield any significant relationships to memory, within-VAN connectivity or their interaction. Likewise, there were no significant effects of memory, VAN connectivity or their interaction on depression symptom scores in Studies 1 or 2

(Wald χ^2's<3.1, p>0.08). The frequency of comorbidity with major depression, assessed similarly in both studies, did not differ as a function of verbal memory, VAN connectivity or their interaction (Wald χ^2<2.9, p>0.09). In Study 2 we assessed additional psychiatric disorders, but similarly found no significant differences between groups in the frequency of generalized anxiety disorder, panic disorder, social anxiety disorder, or alcohol use disorder (Wald χ^2<1.9, p>0.72). Finally, Study 2 included individuals with traumatic brain injury (TBI), indexed as an episode of head trauma-induced loss of consciousness. The frequency of TBI was nonetheless also not related to memory, VAN connectivity or their interaction (Wald χ^2's<1.4, p>0.24). Finally, we examined the influence of memory, VAN connectivity and their interaction of patients' quality of life on the World Health Organization Quality of Life scale, which has subscales for physical health, psychological health, social relationships and environment. However, no significant effect was observed after correcting for multiple comparisons within each study. As such, it appears that, from a cross-sectional clinical perspective, the cognitive biobehavioral phenotype we have identified within the clinical syndrome of PTSD cannot be distinguished by current symptoms or comorbidities (i.e. clinically "latent"). We therefore next asked whether this phenotype was predictive of clinical outcome when PTSD patients are treated with the best-supported intervention for the disorder – exposure-based psychotherapy.

Determining the clinical significance of impaired verbal memory and poor within-VAN connectivity: treatment outcome prediction

The treatment moderation results presented in the main text were unchanged when either controlling for age or excluding participants >55 years old (F's>20, p's<10^{-7}). The moderation effects were also similarly significant when additionally controlling for any baseline symptom differences by treatment arm ($F(2,82)=27.4$, $p<10^{-8}$), or medication use and demographic variables ($F(2,78)=27.1$, $p<10^{-8}$). There were also no differences in baseline PTSD symptoms, verbal memory impairment or within-VAN fMRI connectivity between the treatment arms (Wald χ^2's<1.9, p>0.17).

In spite of the treatment-moderating effects of verbal memory and within-VAN connectivity, neither memory nor connectivity showed a significant change following PE compared to following WL (Figure S4a and S4b; group x time interactions for memory: $F(2,91)=2.3$, $p=0.11$; connectivity: $F(2,111)=0.02$, $p=0.98$). This is consistent with the expectation that individuals with the greatest impairments in both measures failed to respond to PE, while those without both impairments (who responded well to PE) were already within the healthy range on both measures.

Next, to understand the individual-level predictive value of memory and connectivity, we tested these two variables as potential predictors of treatment outcome (quantified as a binary response variable corresponding to a 50% decrease in symptoms) using support vector machine (SVM) classification with leave-one-out cross-validation within the PE arm only. We found that treatment

response could be predicted at 85% accuracy with a linear SVM (sensitivity 80%, specificity 87%; p=0.009 using 5,000 permutation tests) and at 90% accuracy with a non-linear radial basis function SVM (sensitivity 80%, specificity 93%; p=0.01). SVM's using only memory or only connectivity scores did not predict outcome (accuracies $\leq$65%, p's>0.18). Individual data points for memory, connectivity and treatment outcome can be found in parallel coordinate plots in Figure S5. Notably, as classification of outcome requires an observed post-treatment symptom score, these analyses are thus no longer within the intent-to-treat framework, but are nonetheless informative as they speak to individual outcome prediction.

Study 1

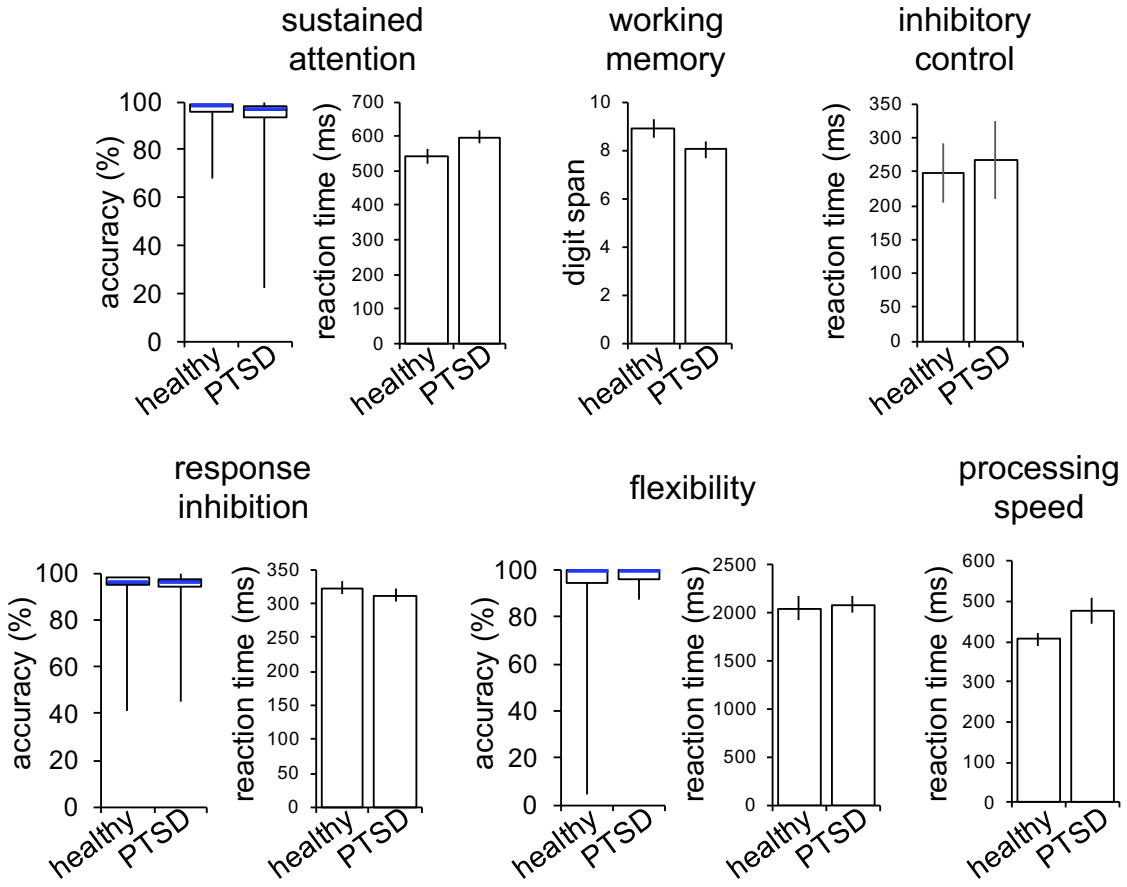

Figure S1: **Neurocognitive task performance in PTSD.** Group comparisons using generalized linear models with appropriate distribution and link functions. Only verbal learning delayed recall survived FDR correction (see Figure 2b). Other domains tested include sustained attention (continuous performance task), working memory (digit span), inhibitory control (color-word Stroop interference), response inhibition (Go/NoGo task), flexibility (trails B task) and processing speed (choice reaction time task). Bar graphs show means and standard errors (for normally distributed variables), while box and whisker plots show medians, interquartile ranges, minima and maxima (for variables with skewed distributions).

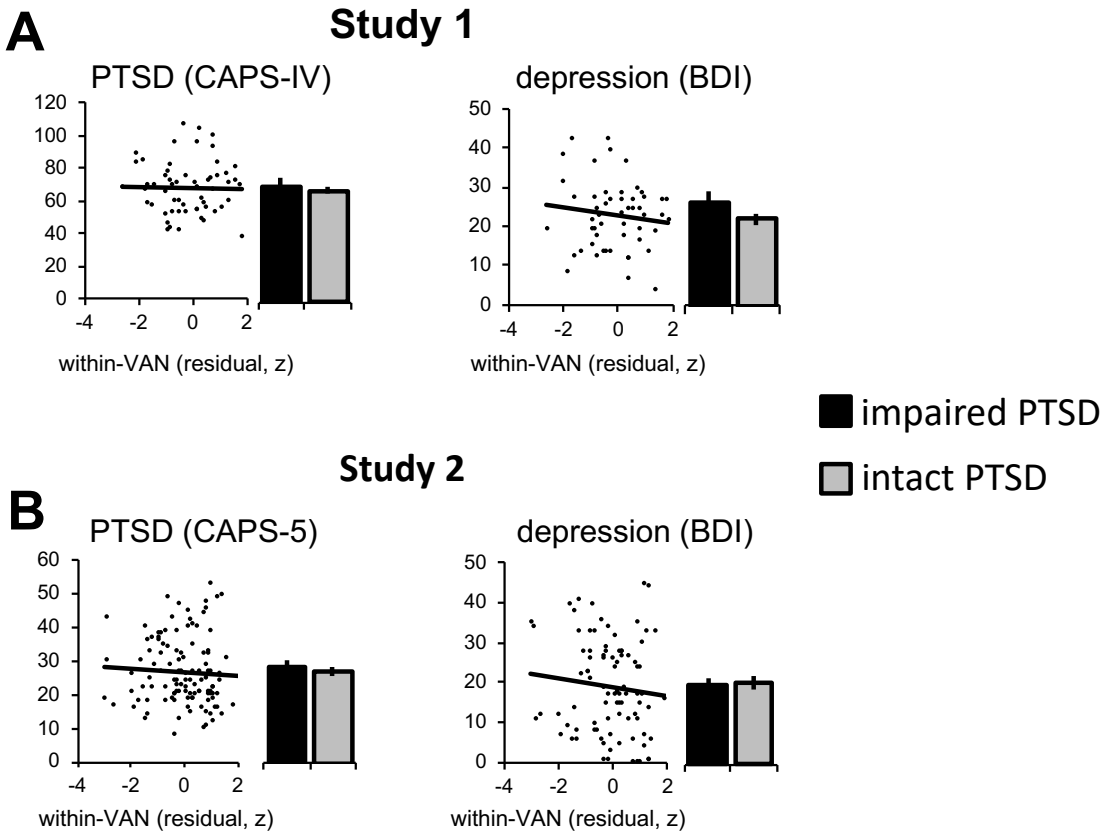

Figure S2: No relationship between the memory/connectivity-related phenotype and symptoms in PTSD patients (Studies 1 and 2). Several aspects of the clinical presentation of PTSD were tested for their relationship to memory impairment, within-VAN fMRI connectivity, or their interaction in the PTSD patients in Studies 1 (A) and 2 (B), but no significant effects were observed. Shown here are overall PTSD symptoms (on the Clinician Administered PTSD Symptoms scale (CAPS)), and depression symptoms (on the Beck Depression Inventory (BDI)). Y-axes on each plot show the value of the scale noted in the title of each plot, as either a scatterplot against within-VAN fMRI connectivity (z-scored residual after regressing out the covariates in the model) or split by memory-based grouping in patients.

Figure S3: **CONSORT diagram for the Study 1 treatment component**

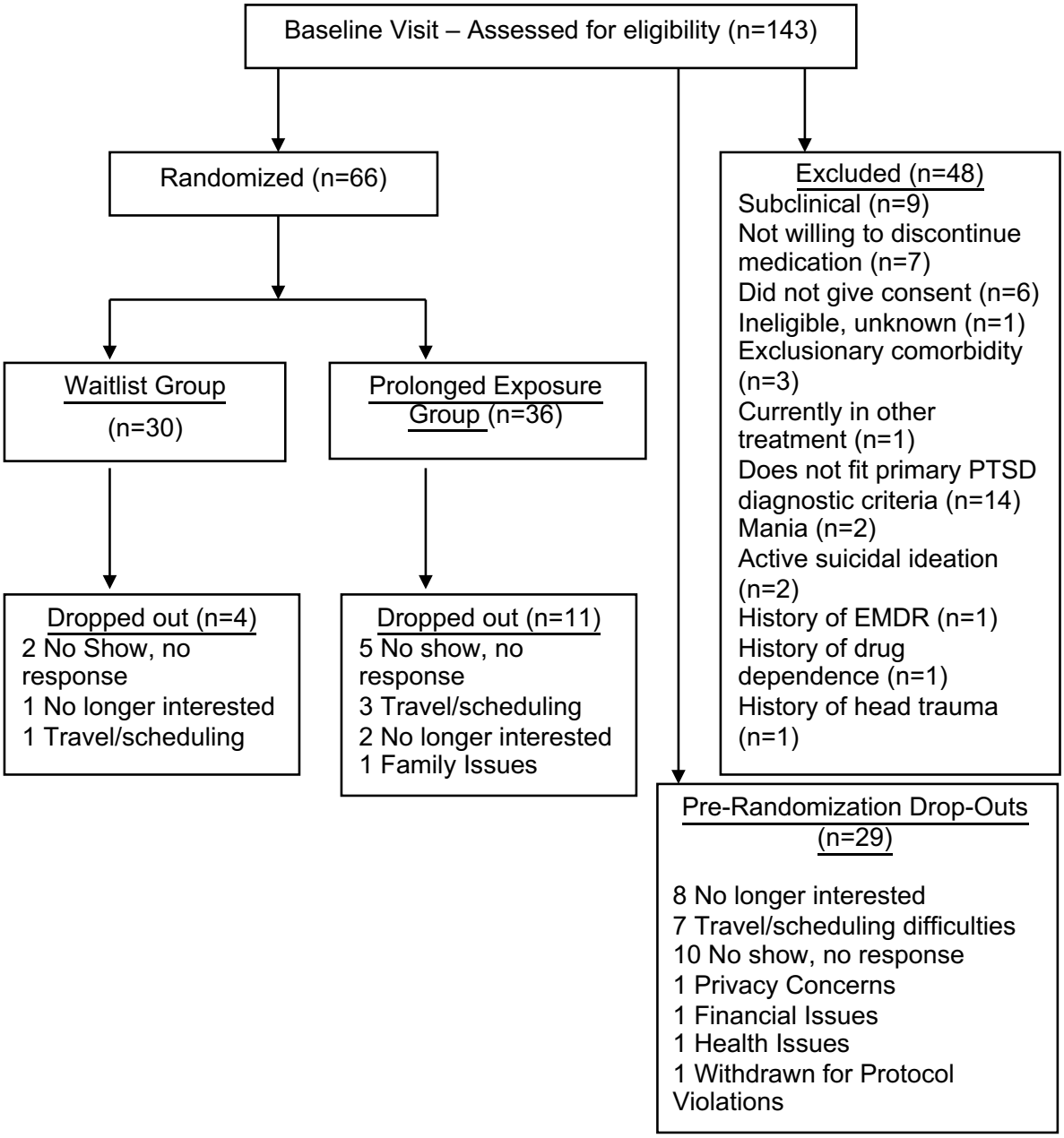

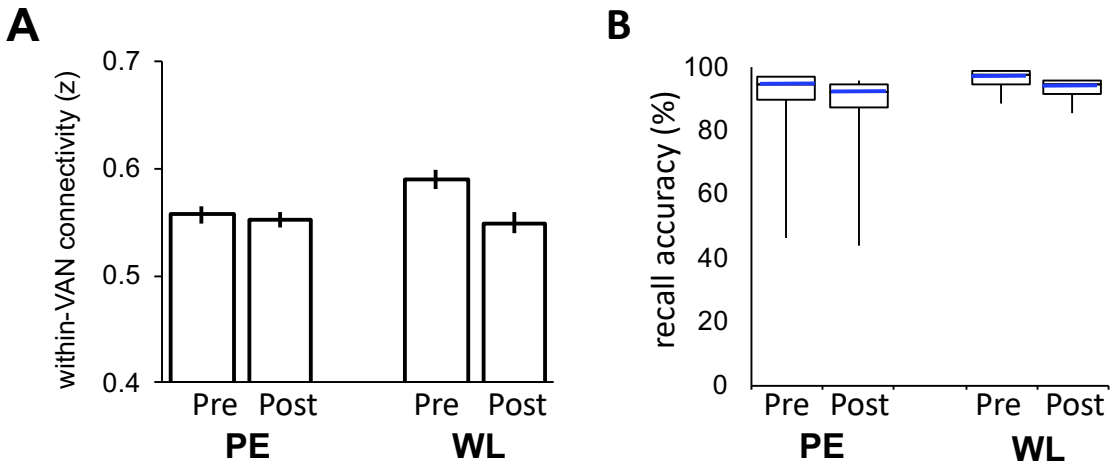

Figure S4: No differential change in either within-VAN connectivity (A) or delayed recall of verbal memory (B) following treatment (i.e. PE versus WL). Bar graphs show means and standard errors (for normally distributed variables), while box and whisker plots show medians, interquartile ranges, minima and maxima (for variables with skewed distributions).

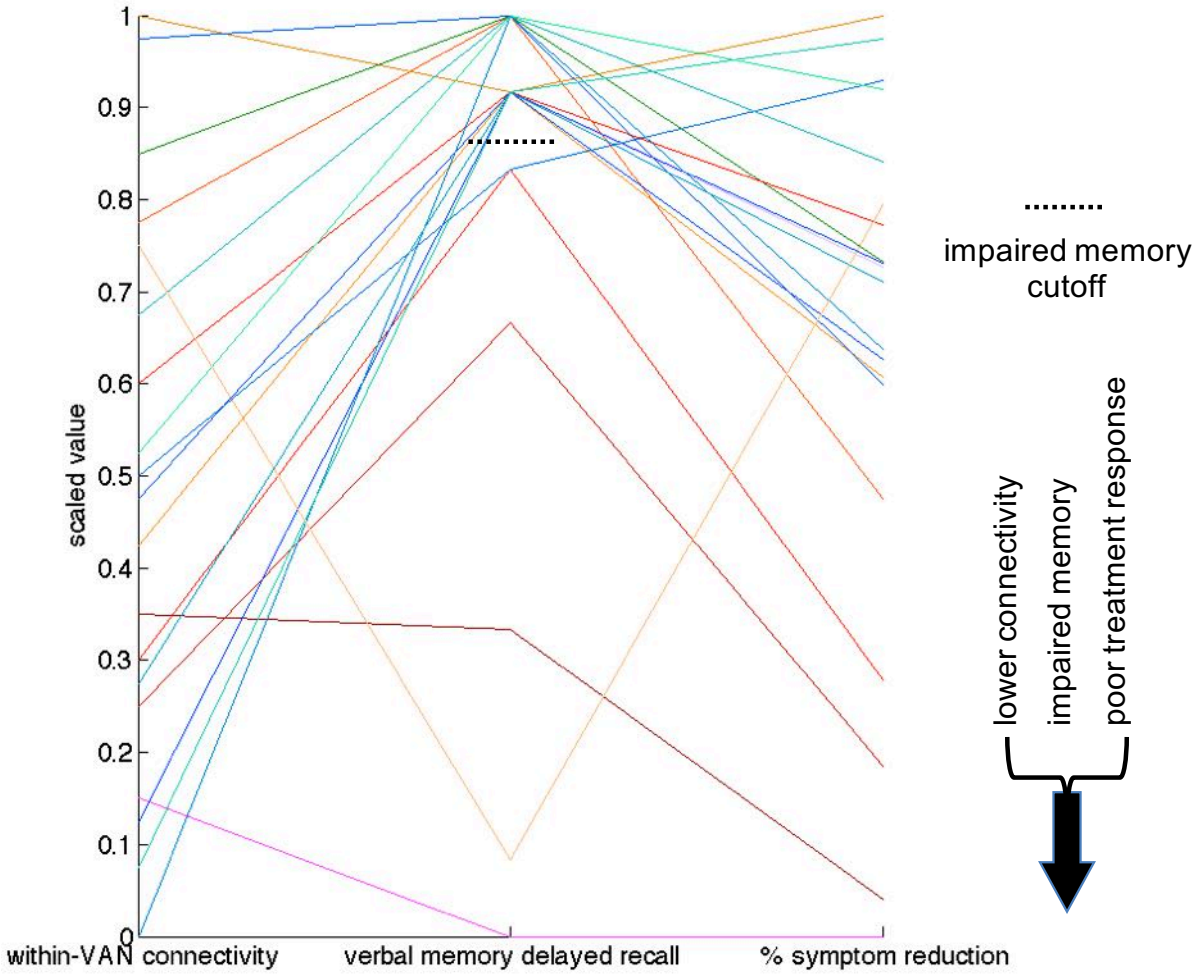

Figure S5: **Individual data points for verbal memory delayed recall, within-VAN fMRI connectivity and percent change in CAPS total scores with treatment in PE arm completers in Study 1.** It is important to note that this plot by necessity only reflects individuals who had each of the moderator variables (fMRI connectivity, memory) and a post-treatment clinical score from which to determine treatment response (here quantified as % symptom reduction). As such, it does not directly reflect the primary statistical testing conducted in the manuscript using linear mixed models in an intent-to-treat framework, and thus is used for illustration purposes only. In order to visualize each of these variables on a common axis, we scaled each of them to a 0-1 range (i.e. (individual value – minimum)/range). Each participant is represented by a different arbitrary color.

Table S1: Demographic and clinical characteristics of participants with means and (standard deviations) for Studies 1 and 2.

	Study 1		Study 2	
	healthy (n=36)	**PTSD (n=76)**	**Healthy (n=117)**	**PTSD (n=128)**
Age (yr)	34.8 (11.8)	36.8 (10.6)	31.9 (7.4)	33.5 (7.4)
Education (yr)	15.3 (2.4)	14.8 (2.5)	15.4 (2.1)	15.2 (2.2)
Gender (% female)	50%	59%	10%	13%
WASI intelligence quotient (IQ)	112.0 (13.7)	110.7 (10.3)	109.2 (11.8)	102.8 (11.1)
Using medications (% yes)	0%	19%	5% (all PRN)	29%
Handedness (% right handed)	100%	100%	89%	90%
self-report				
Beck Depression Inventory	1.5 (1.8)	23.5 (8.5)	4.1 (6.1)	19.0 (11.9)
WHOQOL physical health	88.2 (11.1)	51.1 (19.6)	81.3 (13.2)	60.6 (16.7)
WHOQOL psychological health	75.4 (11.4)	39.1 (14.8)	71.8 (16.0)	51.1 (19.2)
WHOQOL social relationships	76.7 (19.7)	35.9 (23.3)	66.0 (21.3)	50.8 (24.0)
WHOQOL environment	79.8 (14.7)	52.1 (20.8)	72.1 (16.1)	59.1 (16.3)
DSM-IV clinician scales				
CAPS total	1.9 (2.8)	69.1 (15.3)		
CAPS re-experiencing	.4 (1.0)	18.2 (6.2)		
CAPS avoidance	.5 (1.2)	28.3 (8.4)		
CAPS hyperarousal	1.0 (1.7)	22.7 (5.6)		
DSM-5 clinician scales				
CAPS total			3.0 (4.1)	26.6 (10.8)
CAPS re-experiencing			.5 (1.1)	6.3 (3.3)
CAPS avoidance			.2 (.8)	3.4 (1.8)
CAPS hyperarousal			.6 (1.4)	8.5 (5.3)
CAPS negative cognitions			1.7 (2.3)	8.1 (3.5)
Medications or class				
CAPS dissociation	0 (0)	2.0 (2.9)	0.02 (0.2)	0.15 (0.7)
Antidepressant (% yes)	0%	19%	0%	15%
Benzodiazepine (% yes)	0%	0%	0%	6%
Opiate (% yes)	0%	0%	3%	6%
Thyroid (% yes)	0%	0%	0%	1%
Gabapentin (% yes)	0%	0%	0%	3%
Hypnotic (% yes)	0%	0%	2%	11%
Prazosin (% yes)	0%	0%	0%	6%
Mood stabilizer (% yes)	0%	0%	0%	3%
Stimulant (% yes)	0%	0%	0%	2%
Antipsychotic (% yes)	0%	0%	0%	2%

Table S2: Trauma type details for Studies 1 and 2 (percent of PTSD participants endorsing a category for their index trauma).

Civilian/military trauma type (% of patients)	Study 1
Natural Disaster/Fire/Explosion	8.5
Physical Assault	23.7
Assault with Weapon	6.8
Sexual Assault	33.9
Combat/War Zone Exposure	10.2
Injury/Illness/Suffering/Death	16.9

Military trauma type (% of patients)	Study 2
Intentional Use of Force (Torture, Physical Assault)	5.5
Accident (Vehicle – Rollover, Collision)	3.1
Perceived Elevated Threat of Attack	10.2
Small Arms Fire/Fire Fight	18.8
Sexual Assault	3.1
Witnessed a Killed in Action	1.6
Wounded or Dead Bodies/Body Parts	9.4
Explosion	47.7

Table S3: Demographic and clinical characteristics of participants by memory-based groupings.

	Study 1: memory-based grouping (only unmedicated patients)		
	Healthy (n=36)	**Impaired PTSD (n=12)**	**Intact PTSD (n=39)**
Age (yr)	34.8 (11.8)	44.3 (12.2)	33.7 (8.7)
Education (yr)	15.3 (2.4)	15.1 (2.5)	14.8 (2.6)
Gender (% female)	50%	64%	62%
WASI intelligence quotient (IQ)	112.0 (13.7)	107.4 (12.9)	111.4 (9.8)
Using antidepressants (% yes)	0%	0%	0%
self-report			
Beck Depression Inventory	1.5 (1.8)	24.2 (10.2)	22.6 (8.1)
WHOQOL physical health	88.2 (11.1)	46.2 (23.6)	54.9 (17.9)
WHOQOL psychological health	75.4 (11.4)	41.9 (15.5)	39.1 (15.1)
WHOQOL social relationships	76.7 (19.7)	36.0 (27.3)	36.1 (23.4)
WHOQOL environment	79.8 (14.7)	52.0 (25.0)	51.0 (20.7)
DSM-IV clinician scales			
CAPS total	1.9 (2.8)	67.7 (19.5)	67.2 (13.5)
CAPS re-experiencing	.4 (1.0)	17.6 (6.4)	17.8 (5.6)
CAPS avoidance	.5 (1.2)	28.3 (9.4)	27.4 (7.7)
CAPS hyperarousal	1.0 (1.7)	21.8 (6.6)	22.0 (5.0)
CAPS dissociation	0 (0)	1.5 (2.2)	2.1 (3.0)

	Study 2: memory-based grouping		
	Healthy (n=117)	**Impaired PTSD (n=40)**	**Intact PTSD (n=83)**
Age (yr)	31.9 (7.4)	33.9 (5.7)	33.0 (8.0)
Education (yr)	15.4 (2.1)	15.3 (2.4)	15.1 (2.1)
Gender (% female)	10%	5%	16%
WASI intelligence quotient (IQ)	109.2 (11.8)	103.1 (10.8)	102.7 (11.2)
Using medications (% yes)	5% (all PRN)	35%	24%
Handedness (% right handed)	89%	92%	89%
self-report			
Beck Depression Inventory	4.1 (6.1)	18.7 (11.7)	19.1 (12.1)
WHOQOL physical health	81.3 (13.2)	59.5 (14.0)	61.2 (18.2)
WHOQOL psychological health	71.8 (16.0)	50.8 (18.0)	51.4 (20.2)
WHOQOL social relationships	66.0 (21.3)	53.5 (28.3)	49.4 (21.3)
WHOQOL environment	72.1 (16.1)	55.7 (13.8)	60.7 (17.4)
DSM-5 clinician scales			
CAPS total	3.0 (4.1)	27.3 (11.6)	26.2 (10.5)
CAPS re-experiencing	.5 (1.1)	6.9 (3.5)	6.1 (3.3)
CAPS avoidance	.2 (.8)	3.6 (1.9)	3.4 (1.8)

CAPS hyperarousal	.6 (1.4)	8.5 (5.2)	8.4 (5.3)
CAPS negative cognitions	1.7 (2.3)	8.4 (3.3)	8.4 (3.7)
Medications or class			
CAPS dissociation	0.02 (0.2)	0.34 (1.1)	0.05 (0.3)
Antidepressant (% yes)	0%	20%	11%
Benzodiazepine (% yes)	0%	5%	6%
Opiate (% yes)	3%	5%	7%
Thyroid (% yes)	0%	3%	0%
Gabapentin (% yes)	0%	3%	4%
Hypnotic (% yes)	2%	8%	12%
Prazosin (% yes)	0%	3%	6%
Mood stabilizer (% yes)	0%	8%	1%
Stimulant (% yes)	0%	0%	2%
Antipsychotic (% yes)	0%	5%	1%

Table S4: Demographic and clinical characteristics of participants with means and (standard deviations) for the intent-to-treat analysis of treatment outcome and its moderation by verbal memory impairment and within-VAN fMRI connectivity. There were no differences between the groups in any of the baseline characteristics listed below ($p_{uncorrected}>0.05$).

	Study 1 treatment sample	
	prolonged exposure (N=36)	**wait list (N=30)**
Age (yr)	34.4 (10.2)	39.0 (10.4)
Education (yr)	14.7 (2.2)	15.2 (2.8)
Gender (% female)	64%	50%
WASI intelligence quotient (IQ)	109.0 (9.1)	112.8 (11.6)
Using antidepressants (% yes)	17%	20%
self-report		
Beck Depression Inventory (pre)	23.7 (8.7)	23.2 (8.6)
WHOQOL physical health (pre)	52.9 (18.7)	52.7 (19.5)
WHOQOL psychological health (pre)	37.7 (14.3)	42.7 (14.6)
WHOQOL social relationships (pre)	35.7 (25.4)	33.0 (21.9)
WHOQOL environment (pre)	51.9 (21.7)	54.9 (21.1)
DSM-IV clinician scales		
CAPS total (**pre**)	66.3 (15.2)	71.4 (15.0)
CAPS total (**post, completers**)	29.6 (21.2)	64.2 (21.8)
CAPS re-experiencing (pre)	17.5 (6.4)	18.7 (6.0)
CAPS avoidance (pre)	27.0 (7.9)	28.8 (8.9)
CAPS hyperarousal (pre)	21.9 (6.3)	23.9 (4.9)
CAPS dissociation	1.8 (2.6)	1.5 (2.7)

Table S5: Demographic and clinical characteristics of participants in Study 2 who did or did not undergo spTMS/EEG (pooling across healthy and PTSD groups). Shown are means and (standard deviations).

	Study 2	
	No spTMS/EEG (N=121)	**Yes spTMS/EEG (N=124)**
Age (yr)	32.1 (6.9)	33.3 (7.9)
Education (yr)	15.1 (2.0)	15.5 (2.2)
Gender (% female)	14.9%	8.1%
WASI intelligence quotient (IQ)	105.6 (11.0)	106.1 (12.6)
Using medications (% yes)	19%	16%
Handedness (% right handed)	91%	88%
self-report		
Beck Depression Inventory	11.3 (11.9)	12.5 (12.3)
WHOQOL physical health	71.2 (17.9)	70.8 (18.6)
WHOQOL psychological health	63.7 (19.5)	59.6 (21.2)
WHOQOL social relationships	59.6 (22.0)	57.4 (25.5)
WHOQOL environment	66.0 (18.2)	65.3 (16.7)
DSM-5 clinician scales		
CAPS total	15.6 (13.8)	16.4 (15.2)
CAPS re-experiencing	3.8 (3.9)	3.7 (3.9)
CAPS avoidance	1.7 (1.9)	2.3 (2.3)
CAPS hyperarousal	5.0 (5.6)	5.0 (5.7)
CAPS negative cognitions	5.2 (4.2)	5.5 (4.8)